Modelling Iron Floc Filtration Through Porous Media Filters

Additional Master's Thesis

Pieter den Dekker – 4148371

Supervised by:
dr. ir. Doris van Halem
dr. Boris van Breukelen
dr. ir. Ralph Lindeboom

November 2018

Preface

This study examines model iron floc filtration in porous media filters submitted as my additional thesis in fulfillment of the degree requirements of the MSc. in Water Management in Civil Engineering at the Delft University of Technology.

When I began my research several months ago I was little aware of the vast body of superb research readily available on iron oxidation, rapid sand filtration, mathematical modeling of filtration and PHREEQQ. This project taught me much, not only about the subject matter, but my profession as a water engineer, perseverance, and life.

I would like to extend special thanks to dr. ir. Doris van Halem and her team for giving me the opportunity to undertake this research project. I hope this work will contribute in some small way to your mission to make our planet's drinking water free from arsenic contamination. And to dr. Boris van Breukelen, thank you for patiently answering my many questions and assisting me in developing a working model. To dr. ir. David de Ridder, thank you for your input and sharing relevant aspects of your research and experience. Your public service is an example to me.

I would also like to thank my loving wife, Esther, for supporting me throughout the project. Your kind and patient words were much appreciated throughout the process.

Pieter den Dekker

November 2018

Contents

1 Introduction

Groundwater has been a major source of the earth's drinking water for as long as man can remember. In the Netherlands, for example, over 60% of the drinking water is from groundwater. Since groundwater contains iron among other metals, it needs treatment before distributing it to consumer. Iron is removed from groundwater primarily by rapid sand filtration, a robust and reliable technique in use for nearly 200 years. Numerous scientific studies have examined iron removal in porous media filters. But there is still much to learn about the various iron species and processes within these filters. And there is always room for improvement. This study focuses on modeling iron transport through the filtration process. One significant advantage of this modeling is improved treatment of groundwater arsenic contamination.

1.1 Iron in groundwater

Iron is the fourth most abundant element and second most abundant metal in the earth's crust (WHO, 2001). Iron dissolves into groundwater when exposed to organic matter and hydrogen sulfide. It usually exists in two oxidation states, reduced soluble divalent ferrous (Fe^{2+} or iron(II)) and oxidized trivalent ferric (Fe^{3+} or iron(III)). Iron is present in groundwater in different states, depending primarily on the pH and the redox potential (Eh), see figure 1 (Stumm & Morgan, 2012). Because the he pH of groundwater ranges from 5.0 to 8.5, and a redox potential between -0.8 and 0.8 Volts, the water mainly contains ferrous iron, Fe^{2+}. Concentrations vary between micrograms per liter to up to 30 mg/l ferrous iron.

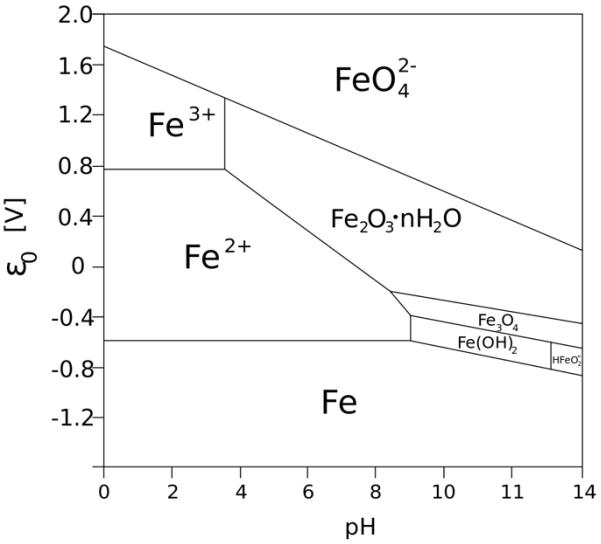

Figure 1 Pourbaix diagram iron in water

Iron in drinking water tastes bitter and causes a brownish discoloration. Furthermore, it adversely affects aspects of the distribution system, and can enhance biological growth, undesirable in some industries.

Accordingly, Dutch drinking water requirements restrict iron content in drinking water to under 0.2 mg/l iron (VEWIN, 2003). WHO recommends a maximum iron concentration of 0.3 mg/ l (WHO, 2001).

1.2 Iron removal

The most prevalent technique to reduce iron concentration in water is rapid filtration through porous media, mainly sand. Different processes and mechanisms occur during the filtration of iron in groundwater into drinking water. The main processes are oxidation, precipitation and filtration.

1.2.1 Oxidation of ferrous iron

Oxidation of ferrous iron can occur by homogenous oxidation, heterogeneous oxidation and biological oxidation. These processes are described in detail in chapter 2.1. Chemical oxidation, by dosing oxidizers is rarely done in practice and therefore not considered in this study.

1.2.2 Filtration of iron flocs

Iron filtration can occur through various ways: mechanical straining, sedimentation, adsorption, chemical activity and biological activity. These processes are further discussed in chapter 2.2.

1.3 Prior research

Iron filtration through rapid sand filters as a field has been studies extensively. The subject can be broken down into three categories: oxidation kinetics of iron, surface complexation modelling and mathematical filtration modelling. Here the main research literature is covered for these subjects that are used in this study.

1.3.1 Oxidation kinetics of iron

Oxidation of ferrous iron has been studied by Weiss, (1934), Stumm et al., (1961), Goto et al., (1971) and Tamura et al., (1976) and Davison et al., (1983). Stumm and Lee elaborated on the kinetic oxidation rates found by Weiss. Tamura, et al. found an empirical formula for the oxidation kinetics of heterogenous oxidation of ferrous iron and Davison and Seed revised these formulae for natural and synthetic waters.

1.3.2 Surface complexation modelling

Sorption of iron on charged surfaces, like an iron floc, has been studied by Dzombak & Morel, (1990). Their study gave insight in the different surface complexation constants of ferrihydrite, an iron floc. This was done through the two-layer model, explained in chapter 2.2.3. Dzombak and Morel incorporated two different kinds of binding sites with, strong and weak affinity for sorption, in their research. Mathur, (1995) however only used one sorption type to fit his cation sorption analysis.

1.3.3 Mathematical filtration modelling of iron flocs

Much research has been conducted on the transport of 'clean' water through porous media, by making use of Darcy's work. However, less research has been done on the filtration of water with suspended solids through porous media. Iwasaki, Slade, & Stanley, (1937) developed a formula, based on the continuity equation, describing the concentration gradient over filter depth as well as filtration time:

$$\frac{\delta C}{\delta z} = -\lambda * C$$

$$\lambda = \lambda_0 + c * S$$

With:

C	concentration of suspended particles at time t and depth z (kg/m^3)
z	the depth of the filter (m)
λ	penetration coefficient that's depending on different filter bed characteristics (m^{-1})
λ_0	starting coefficient (m^{-1})
S	suspended particles left in the filter (kg)
c	coefficient of the penetration coefficient (m^2/kg)

Many researchers have tried to identify an empirical solution for the different parameters. Hall, (1957) described these as 'Interstitial Straining theory'. Ives, (1970) describes the filtration theory purely mathematically and neglects important physical processes involved, like increase in pore flow velocity

and detachment of iron flocs at increased flow velocities. Maroudas & Eisenklam, (1965) extended the formula by describing the 'start-up' process of the filter and the 'catalytic effect' of iron flocs that are already adsorbed by the medium. Tien & Payatakes, (1979) made a comprehensive study of the different filtration dynamics in deep bed filtration. Their research is the gold standard for gravity filtration theory. They made use of Iwasaki's formulae and advanced them and tested them on different filter columns. They were able to synthesize available research from others on the topic and develop a model that predicts deposition and head loss in filter columns.

The aforementioned studies focused on physical and hydraulic aspects of rapid sand filtration rather than changes of water quality due to physio-chemical and biological reactions. However, in their attempt to derive filtration constants these chemical processes are indirectly considered.

1.3.4 Iron removal in rapid sand filtration

Lerck's study, (1965) gives a comprehensive description of the aforementioned topics for rapid sand filtration. In his research he identifies critical parameters respecting filtration of iron flocs and a new empirical solution for the mathematical description of iron floc filtration. Since his research covers most of the rapid sand filtration cycle, it is more easily understood than others. Sharma, (2001) studied the relevant mechanisms that are involved in iron removal by rapid sand filtration. He described the adsorption and oxidation of ferrous iron on the surface of the sand grain particles. His study gives relevant insight in the dominant parameters of these processes.

1.3.5 Filtration modelling

Recently advances have been made to gain more insight in the filtration processes of iron flocs by modelling those in chemical modelling programs like PHREEQC. Vries et al., (2017) performed research on iron and manganese removal, obtaining good results by calibrating the heterogeneous oxidation rates. However, in their model is not able to get proper values for iron in the effluent, it underestimates it. Furthermore, their model assumes a continuous stirred tank reactor (CSTR) as a way to model supernatant water, underestimating the oxygen consumption of homogeneous oxidation.

1.4 Problem definition

Prior research in this area focused on describing and predicting filtration of suspended solids to calculate head losses over the filter. But, there is no model currently available to describe where a specific iron floc is in the filter. This data will be indispensable to help practitioners develop a better picture of the adsorption and desorption kinetics of arsenic on iron flocs in sand filters.

1.5 Objective

The objective of this study is to:

- Build and calibrate a model for the transportation of iron flocs in porous medium filters in order to better identify and understand relevant processes of arsenic adsorption and desorption.
- Provide guidance for future developments of this model.
- Recommend the design of a lab to thoroughly test the model.

PHREEQC will be used to model the aqueous chemistry for the transportation of iron flocs.

1.6 Boundary conditions and focus

There are several constraints for this study.

- *Time*
  The limited ten-week duration of this study made it impossible to comprehensively examine the entire transport mechanism of iron flocs. Therefore, the focus of this study is to first model the basic processes involved in transport of iron flocs, followed by some model enhancement as time permitted.
- *Biological activity*
  Biological activity is a highly significant factor affecting the oxidation and filtration of iron flocs but beyond the scope of this study. Biological activity should be considered in depth once the basics of the iron floc transport model have been shown to work.
- *Definitions*
  It is assumed that the term 'iron floc' is a family name for the various types of iron hydroxides that occur during oxidation and filtration. Hydrous ferric oxide (HFO), ferrihydrite, $Fe(OH)_3$, amorphous ferrihydrite and amorphous iron are different names for the same type of surface. Iron floc transportation and iron floc filtration are used interchangeably herein.

1.7 Research approach

In order to properly build and calibrate a model for the transportation of iron flocs, the different processes involved must first be considered. First, the basic model will be developed based on established filtration theory. The model will be enhanced using unknown parameters that influence the transport of iron flocs, for example, filtration rate coefficients. Use is made of the existing PHREEQC model made by dr. Boris van Breukelen. Iron floc filtration experiments were conducted by dr. David de Ridder. Initially, the model will be calibrated to his data. This will enhance the analysis of different parameters involved and their influence on the transport of iron flocs. Lastly, a sensitivity analysis is done for critical parameters of the model.

1.8 Outline of report

Chapter two explains the theoretical background and application of PHREEQC to the relevant processes. Chapter three describes the experimental set up and lab results of the iron filtration experiments. Chapter 4 gives a description of the adjustments made to the model and its relevant parameters. Chapter 5 summarizes the study, presenting findings and recommendations.

2 Theoretical background and application in PHREEQC

Iron floc transport through porous media filters is affected by different processes. In this chapter the basic processes involved are explained and important parameters are discussed. Additionally, the translation and application into PHREEQC is described. Conclusions are drawn about the importance of the processes and parameters involved.

2.1 Introduction to PHREEQC

PHREEQC is a geochemical modeling program that calculates the equilibrium speciation of solutions based on the thermodynamic constants. It can simulate a variety of reactions and processes in natural water or laboratory experiments. Under equilibrium conditions is can calculate:

- Mixing waters
- Dissolution and precipitation of solid phases
- Effects of changing temperature
- Ion-exchange equilibria
- Surface complexation equilibria
- Solute transport and non-equilibrium calculations

PHREEQC 3, released in 2012, was used in this research.

Keywords

PHREEQC requires an input file that specifies, through easily understandable keywords and data blocks, elements of the problem. First initial solutions are defined, in terms of elemental components (keyword SOLUTION). Next, PHREEQC solves a set of thermodynamic activity and mass-action equations defining a set of 'species' composed from the components present in the solution. These species need not to be aqueous: elements can combine to form solid phases, solid solutions or complexes with surfaces. Here the user can choose which relevant reactions to include in the model. By adding different keywords, such as EQUILIBRIUM_PHASES, EXCHANGE and SURFACE, the processes of respectively the reactions with the mineral, ion-exchange and surface complexation are modeled. Each keyword has its own characterizing parameter that is self-instructive. Once the solution is set and the mass transfer processes to be modeled selected with the keywords, a set of objective functions are defined and solved simultaneously to determine the equilibrium activities for a certain situation.

Basic interpreter

Besides using data blocks to model in PHREEQC, BASIC interpreter can be used to describe different processes and constants in a Linux form, providing different boundary conditions and describing different ways a process can occur. Within BASIC different variables can be used like TIME to have PHREEQC communicate between BASIC and the different data blocks where a timestep is used, for example in KINETICS.

Limitations of the program

Flow in porous media filters occurs within a short time frame (15-30 min.). However, PHREEQC was developed for modelling subsurface chemistry, considering very long timespans for subsurface flows, i.e several years. Since the timeframe for porous media filtration is much shorter, no use is made of the popular Equilibrium function of PHREEQC. Processes are described by using Rates and Kinetics, where one is able to model the chemistry when equilibria is yet to be attained (Appelo & Postma, 2010).

Since PHREEQC was designed for geochemical modelling, physical aspects of the modelling are not considered, unless specifically added in the BASIC interpreter. It is one dimensional and therefore can only give one dimensional output.

The model's limitation is the thermodynamic database forming the bases of the calculation. These databases are based on a variety of literature sources and, at times, are mutually inconsistent.

Furthermore, when modelling iron flocs and adsorbed flocs need to be distinguished from mobile flocs, PHREEQC is unable to assign surfaces for both types of flocs while the mobile flocs travels through the filter. Therefore, all Fe^{2+} and Fe^{3+} processes are decoupled in the database and new iron species are defined.

2.2 Iron oxidation & precipitation

One of the most important processes in iron floc filtration is the oxidation of ferrous iron. The reaction for the oxidation of ferric iron consists of two half reactions and is as follows:

$$Fe^{2+} \leftrightarrow Fe^{3+} + e^-$$

$$O_2 + 4H^+ + 4e^- \leftrightarrow 2H_2O$$

$$4Fe + O_2 + 2H_2O \rightarrow 4Fe^{3+} + 4OH^-$$

Since ferric iron is practically insoluble, it will readily hydrolyze into a hydroxide (iron floc), following the next reaction (Lerck, 1965):

$$4Fe^{3+} + 4OH^- + 2(x+1)H_2O \rightarrow 2(Fe_2O_3 x H_2O) + 8H^+$$

Sharma (2001) described the entire family of possible iron flocs by:

$$Fe^{3+} + mH_2O \leftrightarrow Fe(OH)_m^{(3-m)} + mH^+$$

Iron oxidation can take place in two different ways, depending on the environment it is in, homo- and heterogeneous oxidation.

2.2.1 Homogeneous oxidation

Homogeneous ferrous iron oxidation can be described by the following rate law:

$$-\frac{d[Fe(II)]}{dt} = k * [Fe(II)] * pO_2 * (OH^-)^2$$

Where:

d[Fe(II)]/dt	rate of ferrous iron oxidation (mol l^{-1} min^{-1})
k	rate constant = $8.0 \cdot 10^{13}$ (l^2 mol^{-2} atm^{-1} min^{-1})
pO2	partial pressure of oxygen (atm) = 0.21 $[O_2]/[O_{2\text{-}sat}]$
[O2], [O2-sat]	actual and saturated concentration of oxygen (mol/l)
[Fe(II)]	concentration ferrous iron (mol/l)
[OH-]	concentration of hydroxyl ions (mol/l)

As can be seen in figure 2, the rate law is very pH dependent, increasing a hundred-fold, with a pH increase of one unit.

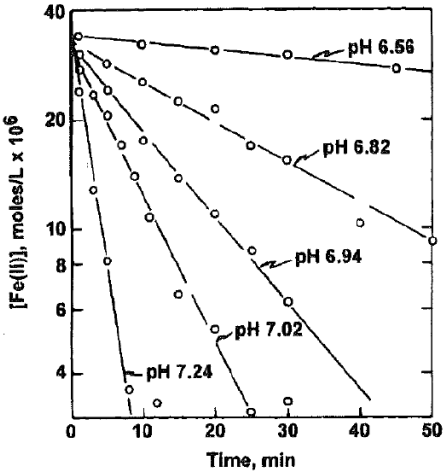

Figure 2 Oxygenation rate of ferrous iron depending on pH (Stumm and Lee (1961).

2.2.2 Heterogeneous oxidation

Ferrous iron can also oxidize directly onto the surface of iron hydroxides. This process is called heterogeneous oxidation and can be described by the following rate law:

$$-\frac{d[Fe(II)]}{dt} = (k + k' * [Fe(III)] * [Fe(II)])$$

With:

k rate constant for homogeneous reaction = $k_0[O_2][OH^-]^2$
$k_o=2.3\cdot10^{14}$ ($l^3mol^{-3}s^{-1}$)

k' rate constant for heterogeneous reaction = $k_{so}[O_2]K[H^+]^{-1}$
k_{so} = 73 ($l\ mol^{-1}s^{-1}$)
K = equilibrium constant for adsorption of ferrous iron on a iron hydroxide, determined by Tamura (1976) as $10^{-9.6}$ mol^{-1} mg^{-1}

[Fe(III)] concentration ferric iron (mol/l)

The heterogeneous reaction rate is not set, since different values have been empirically found in the range of 0.01 – 73 l $mol^{-1}s^{-1}$ (Davison & Seed, 1983; Stumm & Lee, 1961; Tamura et al., 1976; Vries et al., 2017). This range is large and therefore, the rate needs to be calibrated for.
The catalytic effect of the heterogeneous oxidation becomes noticeable at ferric iron concentrations exceeding 5 – 10 mg/l (Tamura et al., 1976).

2.2.3 Biological oxidation

Ferrous iron can also be oxidized biologically, this is done by different species of iron oxidizing bacteria (IOB). Among these are: Leptothrix ochracea, Gallionella ferruginea, Toxothrix trichogenes, Thiobacillus ferrooxidans and Crenothrix (Kirby, Thomas, Southam, & Donald, 1999; S. Sharma, Petrusevski, & Schippers, 2005). Since this study focusses on the basic oxidation processes first, biological oxidation is not considered at this point.

2.2.4 Application in PHREEQC

Oxidation processes are modeled in PHREEQC using the two half-redox reactions from the database. PHREEQC struggles with these redox reactions when it has to calculate a mobile surface and adsorption onto media. Therefore the Fe(2) and Fe(3) redox equilibrium is inactivated and for all ferrous iron Fe_two is used, for ferric iron Fe_three in the database. Furthermore, Iron_floc is defined in Solution_Master_Species to have mobile flocs as species in the system.

In figure 3 an example is given of this change in the database:

```
#FeOH+2                 1
       Fe_three+3 + H2O =Fe_threeOH+2 + H+
        log_k           -2.19
        delta_h 10.4 kcal
        -gamma  5.0     0.0

#FeOH+                  2
        Fe_two+2 + H2O = Fe_twoOH+ + H+
        log_k           -9.5
        delta_h 13.2 kcal
        -gamma  5.0     0.0

#Fe(OH)3-               3
        Fe_two+2 + 3H2O = Fe_two(OH)3- + 3H+
        log_k           -31.0
        delta_h 30.3 kcal
        -gamma  5.0     0.0
```

Figure 3 Example of decoupled Fe master species

Where:

log K; equilibrium constant defined as:

$$K = \frac{[Fe^{3+}][e^{-}]}{[Fe^{2+}]} = 10^{-13.02}$$

$$\log K = log\,[Fe^{3+}] - pe - log[Fe^{2+}] = -13.02$$

$$pe = -\log\,[e^{-}]$$

delta_h; change of K due to temperature difference defined as:

$$\frac{d\ ln\ K}{dT} = \frac{\Delta H_r}{RT^2}$$

with ΔH_r the reaction enthalpy of the system, net energy lost or gained (kcal/mol).

gamma; determines the activity coefficient (γ_i) based on the ionic strength. This property has three different options:

-gamma 9.0 0.0 When only one parameter is used (the second number is zero) the Debye-Hückel Equation is applied to calculate the activity. The first parameter defines the ion-size in Angstrom (å, which is 10-10m).

Since it cannot be expected that all equilibria conditions are reached within the short span of filtration, use is made of the RATES and KINETICS data blocks. First RATES is used to define the mathematical rate kinetic for both the homo- and heterogeneous oxidation. In KINETICS, formulae are given to describe the oxidation kinetics of both processes, including different kinetic parameters used for transport.

CALCULATE_VALUES

In this data block the different parameters are defined that will be used in the RATES and KINETICS data blocks. This is only done to simplify the commands in the next data blocks, see figure 4.

```
CALCULATE_VALUES
k_homogeneous          ; -start;  10 SAVE    1.33e12    ; -end
k_heteroHFO            ; -start;  10 SAVE    73         ; -end
k_heteroSFO            ; -start;  10 SAVE    73         ; -end
k_flocs_formation      ; -start;  10 SAVE    1          ; -end
k_flocs_filtration     ; -start;  10 SAVE    0.1        ; -end
END
```

Figure 4 CALCULATE_VALUES data block

KINETICS

When equilibria are not reached, kinetics can be calculated with PHREEQC. See figure 5. Kinetics are time dependent reactions that occur until equilibrium is reached and reactions become independent of time (at $t>t_2$). In order to do so, PHREEQC depends on reaction rates, defined in the RATES datablock.

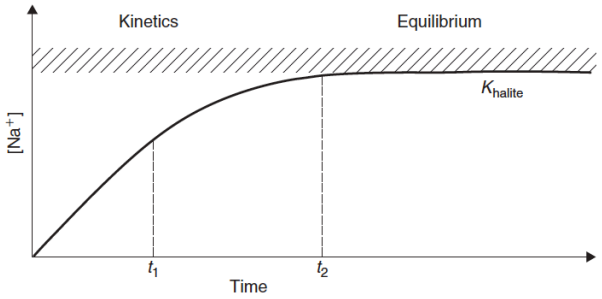

Figure 5 Kinetic and equilibrium states for halite

RATES

Within this data block a mathematical expression of the reaction rates is given for PHREEQC. A simple reaction is considered where compound A is converted to compound B by the reaction:

$$A \rightarrow B$$

This reaction can be followed by recording the concentration of A as a function of time as shown in Figure 6. The reaction rate is the change of A with time. Thus, at time x_1 the rate can be determined from the slope of the tangent. For the whole curve, this is equal to:

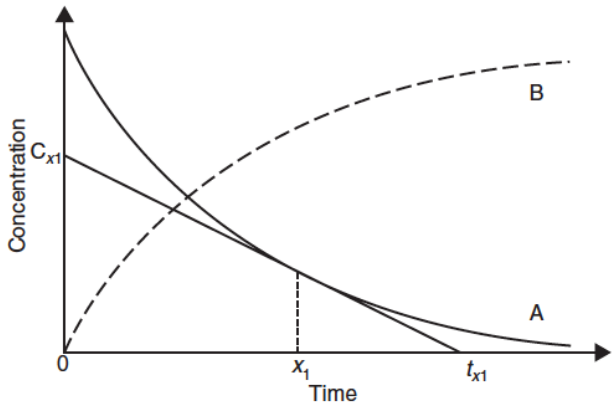

Figure 6 Derivation of rates from concentration/time data

$$rate = -\frac{dc_A}{dt} = \frac{dc_B}{dt}$$

An example of the rate defined for homogeneous oxidation of ferrous iron is given in figure 7 (Appelo & Postma, 2010).

```
RATES
Homogeneous_Iron_Oxidation      # Singer & Stumm, 1970 # Copied from MOSHIUR MODEL
-start
10  Fe_two = TOT("Fe_two")
20  if (Fe_two < 1e-9) then goto 100
30  pP_O2 = 10^(SI("O2(g)"))
40  rate = calc_value("k_homogeneous") * (ACT("OH-"))^2 * pP_O2 * Fe_two
50  if rate > Fe_two then rate = Fe_two
60  if rate > 0.25*mol("O2") then rate = 0.25*mol("O2")
70  put(rate,1)
80  moles = rate*time
100 SAVE moles
-end
```

Figure 7 RATES data block

RATES starts by defining a name for the kinetic function, 'Homogeneous_Iron_Oxidation' in this case. Then a BASIC command is used to define the kinetic function. If Fe_two is smaller than $1.0e^{-9}$ it is considered that no homogeneous iron oxidation occurs. In line 30 the partial oxygen pressure is defined. Line 40 uses the rate defined in chapter 2.2.1. It calls for the "k_homogeneous" parameter defined in the previous CALC_VALUE datablock. The hydroxyl activity is defined as ACT("OH-"). The rate is limited at 0.25*mol [O_2]. In line 80 the concentration is calculated from the rate defined previously and multiplying it by time, the parameter within the BASIC command.

Then in KINETICS the full reaction is described, an example is given in figure 8.

```
KINETICS 0
Homogeneous_Iron_Oxidation
-formula        Fe_two  -1.0  O2 -0.25 H -1 Fe_three  1.0 H2O 0.5
-steps          240
```

Figure 8 KINETICS data block

In KINETICS, the kinetic function used is defined in the RATES data block. It then ascribes a formula to this kinetic rate. The reagents on the left part of the reaction have minus signs, the reagents on the right a positive sign. The numbers behind the reagents are defined by the stoichiometry of this reaction.

2.2.5 Conclusion and discussion

PHREEQC analyzes the oxidation and precipitation of ferrous iron processes in a straight forward manner. The program takes all reactions into account, at the surface, in a complex, or in the solution. It is convenient that these do not need to be defined in advance.

The issue, however, is that there are big differences for the reaction rate constants, especially for the heterogeneous ferrous oxidation. Tamura found that this constant was 73 (l mol^{-1} s^{-1}), however different experimental constants are found between 0.01 and 3.0 (l mol^{-1} s^{-1}). A sensitivity analysis was performed for this parameter. See chapter 4.2.

2.3 Filtration

After ferrous iron is oxidized into ferric iron and hydrolyzed into iron flocs, these flocs and ferrous iron are retained in the filter through different processes. Fundamental filtration models focus on the accumulation of colloids on the single collector (filter grain). Whereas phenomenological filtration models focus on the increase of mass within the differential element. Mathematical theory on filtration is characterized with its different processes and assumptions included. Finally, the conversion of these processes into PHREEQC is examined.

2.3.1. Fundamental filtration models

Fundamental filtration modelling assumes a filter grain as a single collector for particles. From there models are made to describe in what ways particles are attached (collected) to these filter grains. Eventually an estimation can be done for the collection efficiency of the filter, by adding all the single collectors together.

Although they assist with conceptual understanding, fundamental filtration models are not very effective at quantitatively predicting the effluent turbidity in actual full-scale filters for the following reasons: (1) the models are based on an idealized system in which spherical particles collide with spherical filter grains; (2) the hydrodynamic variability and effect on streamlines introduced by the use of angular media are not addressed; (3) the models predict a single value for the filtration coefficient, which does not change as a function of either time or depth, whereas in real filters the filtration coefficient changes with both time and depth as solids collect on the media; and (4) the models assume no change in grain dimensions or bed porosity as particles accumulate. For these reasons, fundamental depth filtration models are often called clean-bed filtration models, and experimental validation generally focuses on the initial performance of laboratory filters (with spherical particles and media grains).

The basic model for water treatment purposes was presented by Yao (Yao, Habibian, & O'Melia, 1971). The transport efficiency η and the attachment efficiency α are ratios describing the fraction of particles contacting and adhering to the media grain, respectively, as described by the equations:

$$\eta = \frac{particles\ contacting\ collector}{particles\ approaching\ collector}$$

$$\alpha = \frac{particles\ adhering\ to\ collector}{particles\ contacting\ collector}$$

The mass flow of particles approaching the collector is the mass flux through the cross-sectional area of the collector:

$$Mass\ flow\ to\ one\ collector = vC\frac{\pi}{4}{d_c}^2$$

With:

v	superficial flow velocity [m/s]
C	concentration of particles [mg/l]
d_c	diameter of collector (grain) [m]

The number of collectors in the control volume must be determined, which is the total volume of media within the control volume divided by the volume of a single collector:

$$Number\ of\ collectors = \frac{(1-p)A\Delta z}{(\pi/6){d_c}^3}$$

WithL

p porosity [-]
A cross-sectional area of filter bed [m^2]
z incremental unit of depth in filter [m]

The mass balance can then be written as:

$$\left(vC\frac{\pi}{4}{d_c}^2\eta\alpha\right) * \frac{(1-p)A\Delta z}{\left(\frac{\pi}{6}\right){d_c}^3} = QC_z - QC_{z+\Delta z} = -vA(C_{z+\Delta z} - C_z)$$

With Q the discharge in m^3/s.

By assuming Δz goed to 0 and the parameters η, α and d_c are constant over depth, the following expression is obtained.

$$C = C_0 \exp\left[\frac{-3(1-p)\eta\alpha L}{2d_c}\right]$$

With:

L Total length of the filter [m]
C_0 Initial concentration [mg/l]

According to Yao, different mechanisms influence the transport to the media surface and attachment to the surface, these include interception (a), sedimentation (b) and diffusion (c), see figure 9.

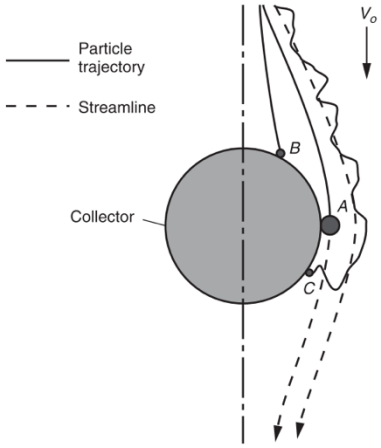

Figure 9 Transport and attachment mechanisms

2.3.1.1 Interception

Mechanical straining or interception is the coarsest physical filtration phenomenon that occurs in porous media filtration. It removes suspended particles that too large to pass through the openings between the media grains, see figure 9. As such it takes place at the surface of the filter bed, i.e. the first few centimeters. Some particles may be trapped in converging spaces (interstitial straining), while the twisting of the water movement causes velocity gradients, bringing the suspended particles in contact with each other. This causes aggregation into bigger flocs and these will be retained deeper in the filter. In rapid filtration, mechanical straining removes a negligible part of the suspended load (Huisman, 2004).

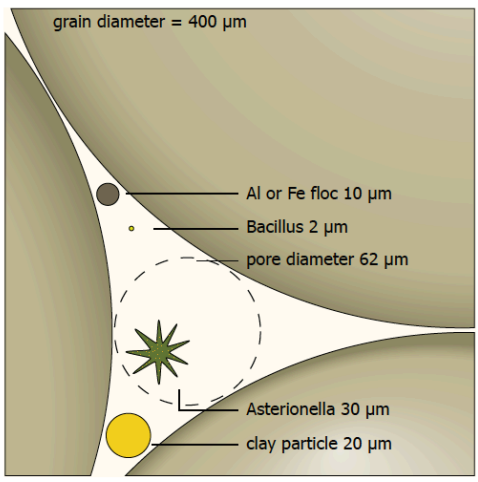

Figure 10 Size of pore openings and suspended particles

For laminar flow, spherical particles, and spherical collectors, particle transport by interception is given by the following expression:

$$\eta_I = \frac{3}{2}\left(\frac{d_p}{d_c}\right)^2$$

With

η_I transport efficiency due to interception [-]

d_p diameter of particle/floc [m]

2.3.1.2 Sedimentation

Sedimentation removes particulate suspended matter of sizes smaller than the pore openings by precipitation upon the grain surface. This occurs in the same way sedimentation occurs in a settling tank. In normal settling tanks, sedimentation occurs only at the surface of the bottom, now in principle the combined surface area of all filter grains is available. With a porosity p (-) and diameter d (m) of the filter material, the combined surface area (m^2) equals:

$$\frac{6}{d}(1-p)$$

The gross area can amount to no less than 4500 m^2 surface area per m^2 surface area of the filter, a depth of 1 meter, diameter of 0.8 mm and porosity of 0.4. Even when only a fraction of this area is effective (facing upward, not in contact with other grains and not exposed to scour) the area of deposition per m^2 of filter bed will easily attain a value of 300 m^2.

Sedimentation efficiency is a function of the ration between the surface loading and the settling velocity of the suspended particle. For laminar settling Stokes gives

$$s = \frac{1}{18} * \frac{g}{\vartheta} * \frac{\Delta\rho}{\rho} * d^2$$

Where:

s	settling velocity (m/s)
g	gravity constant (9.81 m/s^2)
ϑ	viscosity of fluid (m^2/s)
$\Delta\rho\ /\rho$	mass density of suspended particles / water (kg/m^3)
d	diameter of suspended particle (m)

For a filtration flow of 5 m/h the maximum diameter of retained particles by sedimentation equals 11 μm (Huisman, 2004; Ives, 1970). Smaller and lighter particles are only partially removed, although sedimentation efficiency increases with depth. As filtration continues and settled out material decreases pore openings (figure 10), pore velocities will increase and cause sedimentation to stop or even picking up settled material from the bed, taking it deeper into the bed. Since the filter has limited depth, eventually suspended material will appear in the effluent. The system needs to be backwashed, in order to remove all settled material from the grains, to restore purifying capacity.

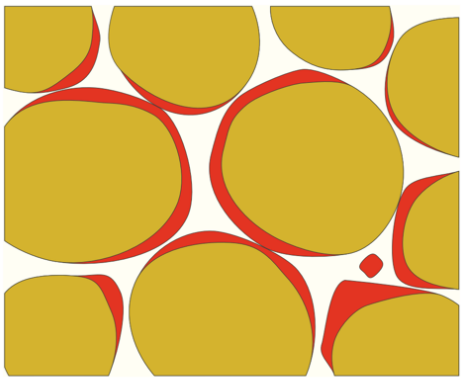

Figure 11 Reduction of pore volume as a result of accumulation of solids (Huisman, 2004)

Particles with a density significantly greater than water tend to deviate from fluid streamlines due to gravitational forces. The collector efficiency due to gravity has been shown to be the ratio of the Stokes settling velocity to the superficial velocity (Yao et al., 1971), as shown in the expression:

$$\eta_G = \frac{v_S}{v_F} = \frac{g(\rho_p - \rho_w){d_p}^2}{18\mu v_F}$$

With:

η_G transport efficiency due to gravity [-]
υ_S Stokes' settling verlocity [m/s]
υ_F Filtration rate (superficial flow velocity) [m/s]

2.3.1.3 Diffusion

Particles move by Brownian motion and will deviate from the fluid streamlines due to diffusion. The transport efficiency due to diffusion is given by the following expression (Levich, 1962):

$$\eta_D = 4\, Pe^{-\frac{2}{3}}$$
$$Pe = \frac{3\pi\mu d_p d_c \upsilon}{k_B T}$$

With
η_D transport efficiency due to diffusion [-]
Pe Peclet number [-]
k_B Boltzmann constant [1.381 × 10^{-23} J/K]
T absolute temperature [K] (273 + ◦C)

The Peclet number is a dimensionless parameter describing the relative significance of advection and dispersion in mass transport. For physically similar systems, a lower value of the Peclet number implies greater significance of diffusion. The formulation of the Peclet number uses the Stokes–Einstein equation to relate the diffusion coefficient to the diameter of a spherical particle. In rapid filtration, diffusion is most significant for particles less than about 1 µm in diameter (Crittenden, 2012).

2.3.1.4 Total transport efficiency

The relative importance of these various mechanisms for transporting the particle to the surface depends on the physical properties of the filtration system. The Yao model assumes that the transport mechanisms are additive:

$$\eta = \eta_I + \eta_G + \eta_D$$

with:
η total transport efficiency [-]

The importance of each mechanism can be evaluated as a function of system properties. The effect of particle diameter on the importance of each mechanism is shown in figure 12. Small particles are efficiently removed by diffusion, whereas larger particles are removed mainly by sedimentation and interception. The Yao model predicts that the lowest removal efficiency occurs for particles of about 1 to 2 µm in size, which has been verified experimentally (Yao et al., 1971).

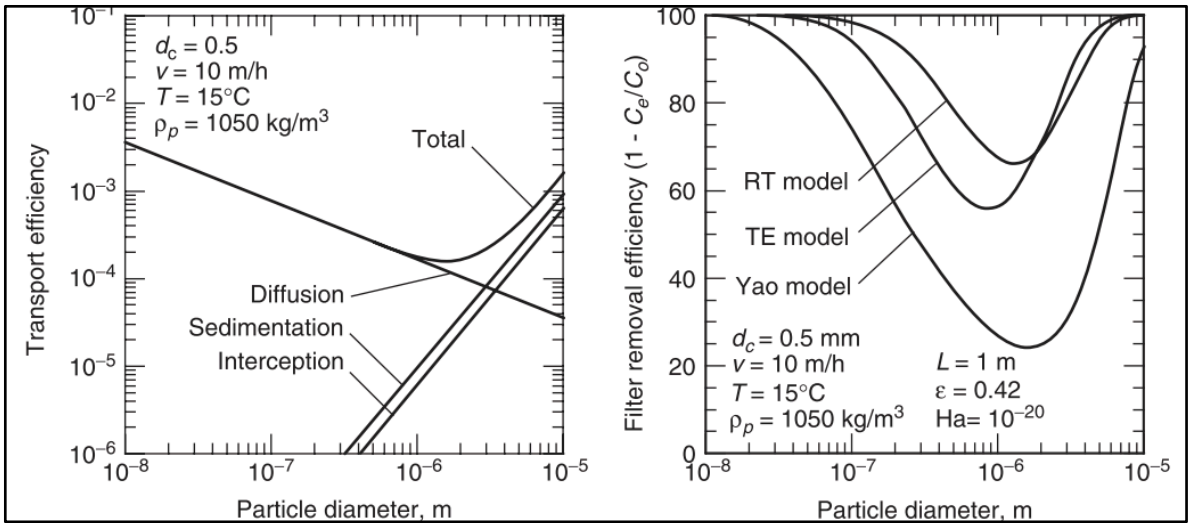

Figure 12 Predictions of fundamental filtration models: (left) importance of each transport mechanism on particles of different size as predicted by the Yao model and (right) comparison of predictions by each model for removal efficiency (Crittenden, 2012)

The Yao filtration model frequently under predicts the number of collisions between particles and collectors when compared to experimental data. Several groups of researchers have tried to refine the Yao model by using a different flow regime or incorporating addition transport mechanisms. Rajagopalan and Tien (1976) developed a fundamental depth filtration model (the RT model) that (1) used a sphere-in-cell model of granular media, (2) accounted for the attraction between the collectors and particles caused by van der Waals forces (for interception and sedimentation only), and (3) accounted for reduced collisions due to viscous resistance of the water between the particle and collector. Following Rajagopalan and Tien's work, Tufenkji and Elimelech (2004) expanded the correlation further (the TE model) and more fully integrated van der Waal forces and hydrodynamic interactions into all transport mechanisms. The RT and TE models are semi empirical expressions that were correlated with the results of a numerical simulation model.

Rajagopalan and Tien:

$$\eta_I = A_s\left(\frac{4}{3}N_a\right)^{1/8} {N_R}^{15/8}$$

$$\eta_G = 0.00338 A_S {N_R}^{-0.4} {N_G}^{1.2}$$

$$\eta_D = 4 {A_S}^{1/3} Pe^{-2/3}$$

$$N_A = \frac{N_{vdW}}{N_R Pe} = \frac{Ha}{3\pi\mu d_p^2 v_F}$$

$$N_{vdW} = \frac{Ha}{k_B T}$$

Tufenkji and Elimelech:

$$\eta_I = 0.55 A_s {N_A}^{1/8} {N_R}^{1.675}$$

$$\eta_G = 0.22 {N_R}^{-0.24} {N_{vdW}}^{0.053}$$

$$\eta_D = 2.4 {A_S}^{1/3} {N_R}^{-0.081} {N_{vdW}}^{0.052}$$

$$\gamma = (1-\varepsilon)^{1/3}$$

$$A_S = \frac{2(1-\gamma^5)}{2-3\gamma+3\gamma^5-2\gamma^6}$$

With:

Ha Hamakers constant [J]
D_L diffusion coefficient [-]

2.3.1.3 Adsorption

Physical process of adsorption

Adsorption is the main purification process for porous media filtration. Purification by adsorption is only possible when impurities are transported into the vicinity of the surface (<1 μm). These transportation processes are: gravity, inertia, diffusion, hydrodynamic forces and turbulence, see figure 11.

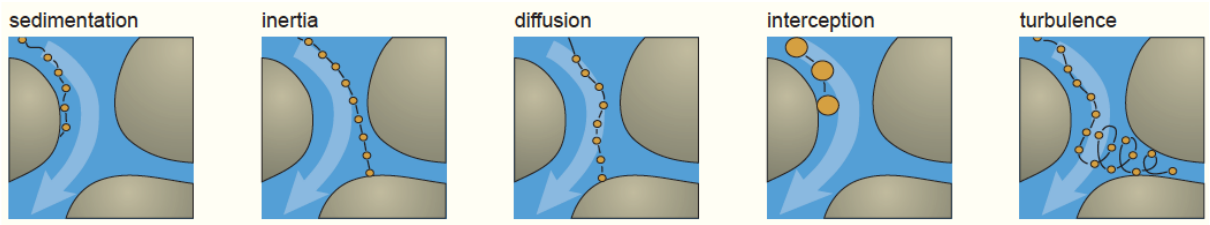

Figure 13 Transport of impurities towards the grain (Huisman, 2004)

It is important to note that a distinction needs to be made between two adsorption processes. The first one is adsorption of iron flocs onto filter media, the second adsorption of ferrous iron onto iron flocs causing aggregation. Main processes involved with adsorption are the physical attraction of particles by the London – Van der Waals' forces and the electrostatic attraction between opposite electrical charges, i.e. Coulomb forces. Sand has a negative charge due to its form and structure and attracts positively charged suspended matter and colloids as well as cations like Fe^{2+}. During filtration parts of these sand grains can become oversaturated with positively charged compounds and are therefore able to sorb negatively charged compounds to them, called secondary adsorption. When secondary adsorption leads to oversaturation, positively charged particles are able to adsorb to the surface again. This process of reversing potential occurs continually and simultaneously, each area of filter grain perpetually changing its charge. During this process however, the magnitude of the charge decreases, lowering the forces of adsorption and efficiency of filtration. This eventually causes the impurities to break through the filter bed, reaching the effluent. Here backwashing is needed also as a way to restore purification capacity.

Chemical process of adsorption

Sorption of ferrous iron occurs when it encounters a charged surface as mentioned before. Adsorbed ferrous iron can then oxidize into ferric iron and new ferrous iron can adsorb on this ferric iron and amorphous iron hydroxides, see figure 12 (S. K. Sharma, 2001).

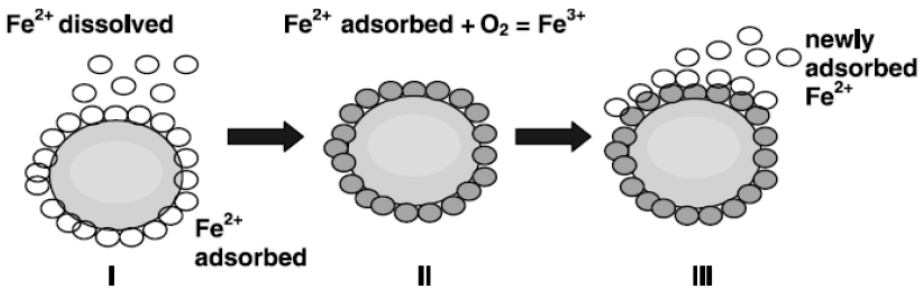

Figure 14 Adsorption - oxidation mechanism (Sharma, 2001)

Iron flocs, or hydrous ferric oxide are covered with surface hydroxyl groups in aqueous environments. The acid-base equilibrium of a hydroxylated oxide surface can be represented as:

$$\equiv S - OH_2^{+} \equiv S - OH + H^{+} \qquad K_{a1}$$

$$\equiv S - OH \quad \equiv S - O^{-} + H^{+} \qquad K_{a2}$$

With $\equiv S - OH_2^{+}, \equiv S - OH, \equiv S - O^{-}$ being the positive, neutral and negatively charged surface hydroxyl groups and K_{a1} and K_{a2} the respective acidity constants. The adsorption of a metal ion on an oxide surface involves the formation of bonds of the metal ion with the surface oxygen atoms and the release of protons from the surface.

$$\equiv S - OH + M^{2+} = \equiv S - OM^{+} + H^{+} \qquad K_m$$

$$K_m = \frac{[\equiv S - OM^{+}] + [H^{+}]}{[\equiv S - OH] + [M^{2+}]}$$

With M^{2+} representing a divalent metal and K_m the surface complexation constant. The rate and capacity of adsorption are affected by the physicochemical nature of the filter media, especially the specific surface area and the surface chemistry (nature of the surface, zeta potential and charge characteristics).

Modelling adsorption: Surface complexation modelling

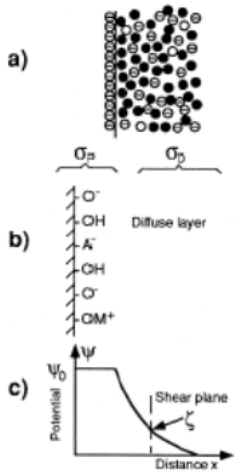

Figure 15 Diffuse Double Layer Model (Drever, 1997). σ_P represents the net surface charge and σ_D the diffuse ion charge (b). (c) shows the distribution of electrical potential ψ.

In order to model adsorption of ferrous iron a detailed description is given for the processes involved at the surface is given; the so-called 'surface complexation'. This theory forms the basis for all calculations on adsorption reactions. Different models were developed. The best known are the 'two-layer' modal and the 'triple-layer' model. Even though the triple-layer model has more flexibility to describe mechanistic details of adsorption, the two-layer model has become the standard for modelling purposes, see figure 13. This is due to the fact that Dzombak and Morel used this model from Gouy-Chapman to extensively research sorption on iron flocs, generating a database for sorption of different ions on iron flocs (Appelo & Postma, 2010). Therefore, PHREEQC adapted this approach to model sorption processes.

Sharma compiled a list of different parameters and processes influencing adsorption of ferrous iron, see figure 14.

Characteristics of filter media	Nature of adsorbate	Water Quality	Others
1. Type of media 2. Surface area - Particle size - Porosity - Density 3. Chemistry of surface - Surface charge - Surface site density 4. Nature of the coating - Mineral form - Crystal structure - Time in use	1. Solubility 2. Surface charge 3. Molecular weight 4. Size of the adsorbate molecule	1. pH 2. Other adsorbates 3. Ionic concentration 4. Alkalinity 5. Organic matter 6. Temperature	1. Filtration rate 2. Rate of regeneration of adsorption sites

(Compiled from Weber 1972; Faust and Aly 1983; Dzombak and Morel 1990; Stumm and Morgan 1996)

Figure 16 Factors affecting adsorption on filter media (Sharma, 2001)

Ferrous iron adsorption on iron hydroxides

Iron flocs exist in different mineralogical and morphological form. Of the many known today, four are commonly found in the iron removal process: lepidocrocite (y-FeOOH), amorphous iron(III) hydroxide ($Fe_20_3.H_20$) and ferrihydrite ($Fe_5H0_8.4H_20$) (Tamura et al. 1976; Sung & Morgan, 1980; Robinson, Baumann, & Demirel, 1981; Carlson & Schwertmann, 1980). Characteristics of these flocs depend on water quality and filtration conditions. They will age over time and form more steady end-products. The occurrence, formation, transformation and pathways of different iron (hydr)oxides are well researched and documented by Cornell and Schwertman (Cornell & Schwertmann, 2003).

In this study amorphous iron(III)hydroxide (HFO) is considered to be the main iron floc in the process. This is done, since Dzombak and Morel and Apello & Postma used it as the main iron floc in their studies and therefore have their databases build on this type of floc. In table 1 an overview is given on the specifics for HFO.

Parameter			Source
Specific density	[kg/m^3]	3.5	Geissen, 1966
Specific surface area	[m^2/g]	600	Davis, 1977
Specific surface area	[m^2/mol]	53,400	Davis, 1977
Molar weight	[gram/mol]	89	$Fe_20_3.H_20$
Strong sites	[mol sites /mol Fe]	0.005	Dzombak and Morel, 1990
Weak sites	[mol sites /mol Fe]	0.2	Dzombak and Morel, 1990

Table 1 Different parameters for iron flocs

2.3.4 Phenomenological filtration models

Phenomenological models do not focus on the accumulation of particles on a single collector but instead consider the increase of mass within the differential element. The basic mass balance equation for phenomenological models is developed with the following simplifying assumptions: (1) although particles are present in the interstitial fluid and at the surface of the media, the accumulation of particles in the interstitial fluid is negligible compared to the accumulation of particles on the media; (2) the number of particles entering and exiting the element by diffusion is negligible; and (3) the generation or loss of particles due to reaction is ignored.

Iwasaki was the first one describing filtration in a phenomenological way (Iwasaki et al., 1937). After him, Ives performed a benchmark study which others adopted to improve upon (Ives, 1970). Among these scientists were (Bai & Tien, 1996; Elimelech, 1994; Elimelech, Gregory, & Jia, 2013; Jegatheesan, Vigneswaran, Group, & Box, 2007; Johnson & Elimelech, 1995; Maroudas & Eisenklam, 1965; O'Melia & Ali, 1979; Rajagopalan & Tien, 1976; Tien & Payatakes, 1979; Tien, Turian, & Pendse, 1979; Yao et al., 1971). An overview of the most important studies was made by Keir et al. (Keir, Jegatheesan, & Vigneswaran, 2009). It is described in the next part of this chapter §2.4.

2.3.5 Application in PHREEQC

To apply this filtration theory in PHREEQC, use is made of RATES, SURFACE and TRANSPORT. Since TRANSPORT is a very specific topic for this study it is explained in more detail in chapter 2.4. It is important to note that the filtration processes are only occurring in the filter, i.e. not in the supernatant. From the supernatant 'Solution 0' is fed into the filter. First surface needs to be assigned to iron flocs and the filter medium. This is done through SURFACE, see figure X.

```
SURFACE 1-10
Sfo_sOH          5e-6     600     0.09
Sfo_wOH          2e-4
Hfo_sOH          5e-17     600     0.09e-11 Dw 1e-9
Hfo_wOH          2e-15
-donnan 1e-10
-equil  1
END
```

Figure 17 SURFACE data block used within the filter

Due to the fact that surface has to be defined for each transport cell, surface is defined for 1-10. In this model two types of surface are defined, 'Sfo' and 'Hfo'. 'Sfo' is assigned to the surface of the filter medium, 'Hfo' represents the mobile flocs that travel through the filter. Both surface types have strong ('sOH') and weak ('who') surface sites. The first column of values represents the total amount of surface sites (moles), the second represents the specific surface area (m^2/g) and the third the initial concentration in the water (mol/l). 'Dw' is the diffusion factor for the mobile surface, this way the flocs are able to travel through the filter. 'Donnan' is used to tell PHREEQC how thick the Donnan layer needs to be modeled and 'equil' is used afterwards to tell that the solution is in equilibrium with the first cell of the column.

With the KINETICS block all the different kinetic reactions are described that are occurring in the filter column, see figure X.

```
KINETICS 1-10
Homogeneous_Iron_Oxidation
-formula        Fe_two  -1.0  O2 -0.25 H -1 Fe_three  1.0 H2O 0.5
Heterogeneous_Iron_Oxidation_HFO
-formula Hfo_wOFe_two+ -1.0     O2 -0.25        H2O -2.5        Fe_three(OH)3 1.0       Hfo_wOH 1.0     H 1.0
Heterogeneous_Iron_Oxidation_SFO
-formula Sfo_wOFe_two+ -1.0     O2 -0.25        H2O -2.5        Fe_three(OH)3 1.0       Sfo_wOH 1.0     H 1.0
Formation_Iron_Flocs
-formula        Fe_three(OH)3 -1        Iron_floc 1             Hfo_wOH 0.2 Hfo_sOH 0.005
Filtration_Iron_Flocs
-m0 0
-formula Iron_floc 1 Hfo_w 0.2 Hfo_s 0.005 Sfo_w -0.2 Sfo_s -0.005
END
```

Figure 18 KINETICS data block used within the filter

In the KINETICS data block all relevant formulae are defined, see chapter 2.2. With 'Formation_Iron_Flocs' iron flocs are generated after the oxidation reactions and weak and strong surfaces are assigned. 'Filtration_Iron_Flocs' has an initial starting concentration of zero, represented by m0=0. It is important to note that the assigned mobile surfaces on the left part of the reaction have positive signs, the surfaces on the right a negative sign.

2.3.6 Conclusion and discussion

It is difficult to use PHREEQC as a basis for modelling filtration. Since there are different processes that need consideration and PHREEQC was not build to describe these in detail, it is not used to model mobile flocs that travel through a column, while at the same time being involved in different reactions.

It is important to note that in this model only one type of iron floc is used, whereas in reality there are at least 4 different types of iron flocs, all with their own site density, surface area and different site types. Furthermore, it is observed that there is quite some discussion in literature on the exact values to characterize the surface of these different iron flocs (site density, surface area, different site types). When a model can simulate different iron flocs and has more detail in the different media that can be used this would really enhance the filtration model.

Lastly, it is concluded that the relation of the specific surface area is not as straight forward as it was expected based on the theoretical background. It turns out that it has a rather complex relation to different mechanisms in the model.

It is recommended to study the relation of specific surface areas of different iron flocs more closely in the future and it is advised that PHREEQC should be expanded with more in-depth parameters to model for different iron flocs and different filter media.

2.4 Transport

In this chapter the relevant processes and steps are explained which are involved in the transport of suspended solids in porous media. First the general transport theory is explained after which a mathematical description is given for the transport of particles within a filter.

2.4.1 General transport theory

PHREEQC has the capability to model several one-dimensional transport processes including: (1) diffusion, (2) advection, (3) advection and dispersion, and (4) advection and dispersion with diffusion into stagnant zones. All these processes can be combined with equilibrium and kinetic chemical reactions. Conservation of mass for a chemical that is transported yields the advection-reaction-dispersion (ARD) equation, see figure 17:

$$\frac{\delta C}{\delta t} = -v\frac{\delta c}{dx} - \frac{\delta q}{\delta t} + D_L\frac{\delta^2 c}{\delta x^2}$$

With:

C	concentration in water (kg/m^3)
t	time (s)
v	flow velocity (m/s)
x	distance (m)
D_L	hydrodynamic dispersion coefficient (m^2/s) $D_L=D_e+\alpha_L \cdot v$
D_e	effective diffusion coefficient (m^2/s)
α_L	dispersivity (m)
q	concentration of suspended matter in pore volume (kg/m^3)

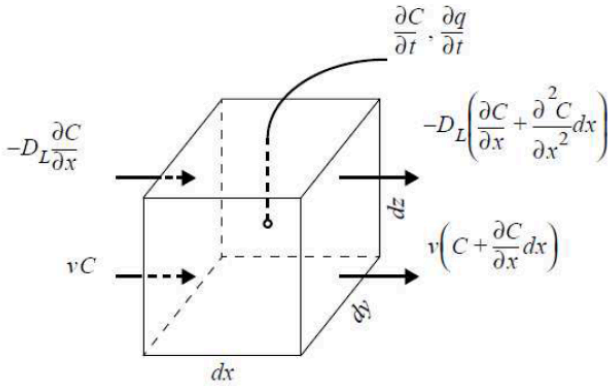

Figure 19 Terms of the ARD equation (Parkhurst and Appelo 2012)

The first term in the ARD equation represents the advection. The second is the reaction term representing the change in concentration of the solid phase due to reaction. The last term represents the dispersion in the system.

2.4.2 Phenomenological transport theory

When the general transport theory is applied to filtration columns different assumptions have to be made: filter consists of spherical grains with a uniform diameter d_0, and porosity p_o.

During filtration impurities from the raw water are transferred to the filter grain surfaces. Therefore, the amount of impurities in raw water c_o decreases over increasing to c at a depth y, eventually reaching c_e at the filter bottom, where y=L. At the same time, d_o increases to d at a depth y and p_o will decrease to p. With v as constant rate of filtration, real velocities inside the pores of the filter bed thus increase from v/p_o to v/p. It is assumed that the decrease of impurities carried by the flowing interstitial water is proportional to the concentration still present (Fick's law).

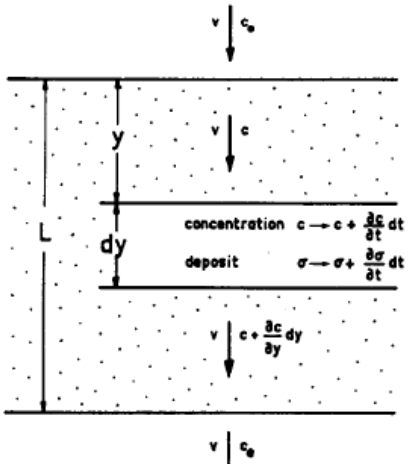

Figure 20 Improvement in water quality (Huisman, 2004)

The assumptions that are made are: (1) the specific deposit is averaged over the entire filter bed, (2) solids accumulate at a steady rate over the entire filter run (the reduced

accumulation of solids during ripening is ignored, under the legitimate assumption that the relatively small quantity of solids retained in the bed during ripening has little impact on the specific deposit over the entire filter run), and (3) head loss increases at a constant rate. Resulting in the variation of concentration of suspended and colloidal solids, which is given by:

$$\frac{\delta c}{\delta t} = -u\frac{\delta c}{\delta y} - \lambda uc$$

Since the concentration changes strongly with depth, but little over time further simplification is made to:

$$-\frac{\partial c}{\partial y} = \lambda c$$

With λ as proportionality coefficient or coefficient of filtration (m^{-1}) and c being the concentration of the suspended particle (kg/m^3)

The equation of continuity based on figure 18 is written as:

$$in = out + storage + deposition$$

$$v \cdot c \cdot dt = v\left(c + \frac{\delta c}{\delta y}dy\right)dt + p\frac{\delta c}{\delta t}dtdy + \frac{\delta \sigma}{\delta t}dtdy$$

Simplified:

$$\frac{\delta \sigma}{\delta t} = -v\frac{\delta c}{\delta y} - p\frac{\delta c}{\delta t}$$

Since the concentration changes strongly with depth, but little over time further simplification is made to:

$$\frac{\delta \sigma}{\delta t} = -v\frac{\delta c}{\delta y}$$

Where:

σ	gravimetric concentration of impurities (kg/m^3)
v	filtration velocity (m/s)
y	depth of filter (m)

When both equations for continuity and motion are combined one gets:

$$\frac{\delta \sigma}{\delta t} = v\lambda c$$

However, λ depends on different factors, such as the filtration velocity, viscosity, grain size, quality of the raw water, and the clogging of the bed. Maroudas found for the start-up of the filtration process, the filtration coefficient initially increases because of better attachment characteristics on the preloaded material (Maroudas & Eisenklam, 1965). Due to pore clogging, the pore velocity increases and fewer solids accumulate, expressed by a lower filtration coefficient λ. When the solids are retained in the top layer of the filter bed, lower layers will take over until the filter is saturated and the filter breaks through. The clean bed filtration coefficient λ0 and the relationship between λ and σ have to be determined in practice, through column experiments. Several researchers have found empirical relationships, such as those described by Lerck and Maroudas (Lerck, 1965).

Lerck:

$$\lambda_0 = \frac{k_1}{v \cdot \vartheta \cdot d^3}$$

Maroudas:

$$\lambda = \lambda_0 \cdot (1 - k_2 \cdot \frac{\sigma_v}{p_0})$$

Where:

λ_0	initial filtration coefficient (m^{-1})
λ	filtration coefficient (m^{-1})
k_1, k_2	filtration constant (-)
v	filtration velocity (m/s)
ϑ	kinematic viscosity ($m^{2/s}$)
σ_v	volume concentration in pores (m^3/m^3)
p_0	initial porosity (-)

Filtration constant k_1=9e-18 and k_2 is the value of reciprocal pore filling n (0<1). For the solution in general this gives:

$$c = c_0 \cdot \frac{e^{\alpha \cdot t}}{e^{\lambda_0 \cdot t} + e^{\alpha \cdot t} - 1}$$

With α defined as:

$$\alpha = \frac{v \cdot c_0 \cdot \lambda_0}{n \cdot \rho_d \cdot p_0}$$

At y=L the effluent concentration becomes:

$$c_e = c_0 \cdot \frac{e^{\alpha \cdot t}}{e^{\lambda_0 \cdot t} + e^{\alpha \cdot t} - 1}$$

And the pore volume concentration becomes:

$$\sigma_v = n \cdot p_0 \cdot \frac{e^{\alpha \cdot t} - 1}{e^{\lambda_0 \cdot y} + e^{\alpha \cdot t} - 1}$$

2.4.3 Dispersion

The spreading of a concentration front is called dispersion. There are two types of dispersion: longitudinal dispersion D_L, differences in travel time around the surface along the flow lines. Transverse dispersion D_T, is due to step over onto adjacent flow lines. For high and low velocities, the dispersion can be calculated by the Peclet number. For high velocities (>1m/week) the effect of dispersion becomes small (Appello and Postma, 2015).

2.4.4 Diffusion

A concentration difference between two points in a stagnant solution will be leveled out in time by the random Brownian movement of molecules. This process is called molecular diffusion. For a detailed description of the theory the reader is referred to Appelo and Postma (2005) paragraph 3.5. Diffusion coefficients D_f for different molecules in free water can be calculated from ionic mobilities. But the

differences in D_f remain small and in most cases, it is sufficient to use the constant diffusion coefficient in free water of 10-9 m^2/s. Since diffusion through a porous medium is different compared to diffusion in free water, solutes must travel an extra distance because they have to circumnavigate the filter grains. The effective diffusion coefficient D_e corrects for the additional pathway. For very small time scales (<days) the effect of dispersion cannot be neglected. Especially in filtration columns it needs to be considered (Crittenden, 2012).

2.4.5 Application in PHREEQC

Transport of solutions and suspended solids is done in PHREEQC through the TRANSPORT data block.

In RATES the filtration rate is described as defined in this chapter, see figure 19.

```
Filtration_Iron_Flocs
 -start
10 if (tot("Iron_floc") < 1e-9) then goto 100
20 rate = -calc_value("k_flocs_filtration") * tot("Iron_floc")
70  put(rate,5)
80  moles = rate*time
100 SAVE moles
 -end
```

Figure 21 RATES data block for filtration

In KINETICS this filtration rate is assigned to every cell in the column as can be seen in the previous chapter.
TRANSPORT is used to transport 'Solution 0' from the supernatant into the filter, see figure 20.

```
TRANSPORT
-cells                  10
-lengths                0.1
-dispersivities         0.001
-diffusion_coefficient  1.295e-9
-shifts                 5
-time_step              10
-flow_direction         forward
-boundary_conditions    flux flux
-punch_cells            1-10
-punch_frequency        5
-print_frequency        2000
-multi_d                true 1e-9 0.3 0 1
```

Figure 22 TRANSPORT datablock

First the supernatant solution is calculated. Here iron flocs are formed due to the kinetic reactions occurring and surface is assigned to these flocs. This solution is then saved as 'Solution 0', ready to be transported into the filter bed. After passing a cell, where the different kinetic, filtration and surface processes take place, the final solution is saved as a new solution. This new solution is then fed into the next cell, and the process is repeated. At the end the final solution, the effluent is reached after transport through six cells.

Six cells are used for the transport process, more would have resulted in even longer calculation times for PHREEQC and fewer would have led to less reliable data over depth. The length of one cell equals

the total column length divided by the number of cells ($\frac{0.4}{6} = 0.0667$m.) Dispersion is set 0.0001 and diffusion set to 1.29e^{-9}.

Shifts determines how many bed volumes are being treated, according to the following formula:

$$BV = \frac{shifts}{cells}$$

In this case three bed volumes are modelled. It takes 54 sec. to travel through one cell with a velocity of 5 m/s therefore, time step is set to 54 sec. The flow direction is set forward, so the solution flows from cell one towards six. Three types of boundary conditions can be applied:

1. constant, the concentration is constant $C(x_{end},t) = C_0$, also known as first type or Dirichlet boundary condition.
2. closed, no flux at boundary, also known as second type or Neumann boundary condition.
3. flux, Flux boundary condition $C(x_{end}, t) = C_0 + \frac{D_L}{v}\frac{\delta C(x_{end},t)}{\delta x}$, also known as third type or Cauchy condition.

Here both boundary conditions are set as a flux boundary condition.

'Punch cells', 'punch frequency' and print frequency' are parameters used for the data output in graphs and tables.

'Multi-d' is used so each solute can be given its own diffusion constant and diffusion rates are defined for the different solutes.

'Correct-disp' corrects for the dispersion of the last half cell. Since PHREEQC calculates each solution at the center of the cell, the effluent concentration misses one half cell simulation. This is corrected with this command.

2.4.7 Conclusion and discussion

Even though PHREEQC was not designed for rapid filtration, it can model reasonably well for this. Chemical and biological filtration processes are considered for mathematical filtration theory. This is caused by the fact that parameters from the theory are made to fit reality and thus including these processes. It is however uncertain to what extant these processes determine the overall filtration rates described in this chapter. Further research is therefore needed to decouple these processes and describe them separately.

3 Lab experiments

Dr. ir. David de Ridder has conducted a laboratory experiment with the goal of gaining a better understanding in the removal of arsenic. His experiment consisted of 6 different filter columns, with three different pH levels. All six columns were triple bed filters, consisting of anthracite, sand and garnet. For his experiment he dosed ferrous iron as well as arsenite. Since he measured iron and arsenic concentrations over the depth of the filter, this data could also be used for modelling iron floc transport through these filters.

3.1 Set up

The lab experiment consisted of 6 different filter columns, with pH ranging from 6.4, 7.1 and 7.8. Experiments were performed in duplo. Filters consisted of, from bottom to top, garnet (0-20cm), sand (20-60cm) and anthracite (60-100cm), having a filter height of 1.0 m. Samples were taken 4 times. One day, 2 days (twice) and 3 days after backwashing of the filter.

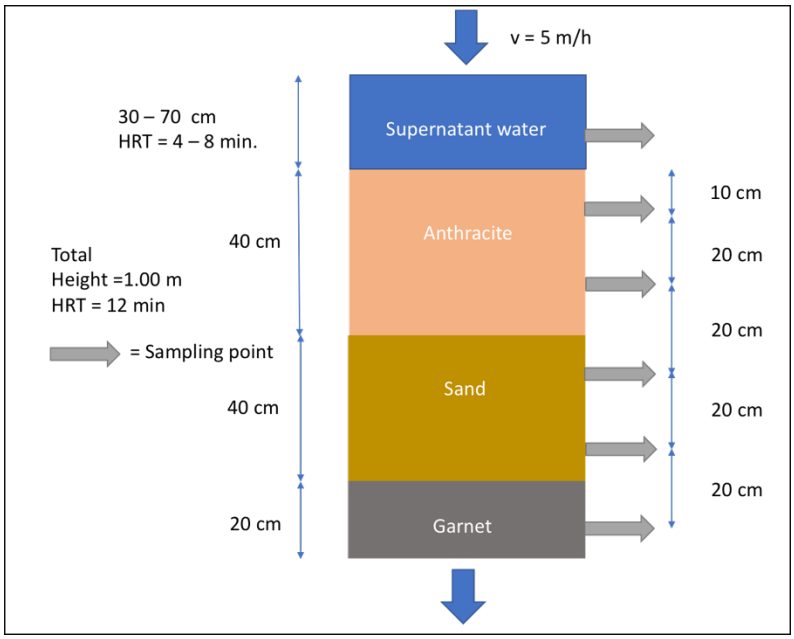

Figure 23 Filtration column set - up

Influent water consisted of fresh drinking water from Evides, see Appendix A. This water had 2 mg/l Fe^{2+} and 20 µg/l As^{3+} dosed to it. Sampling was done at different heights in the bed, see figure 22. Filtrated and unfiltrated iron was measured, sieved through a 0.45 µm screen. The unfiltrated iron content represents the total iron content in the water. The filtrated iron content represents the dissolved iron, consisting only of ferrous iron. When the ferrous iron concentration is subtracted from the total iron content, a measure for iron flocs is obtained. I.e. the particles that were retained by the 0.45 µm screen. It is important to note that this iron floc concentration represents the mobile floc. Mobile flocs are not attached to a grain or filtered out by the filter. However, they have the potential to be adsorbed or filtered in the lower filter layers.

3.2 Results

For this study the top layer anthracite data is used to validate the iron floc transport model. Iron concentrations for ferrous and mobile iron flocs are measured from this layer, see figure 23 and 24. As expected, results show a significant decrease in iron floc content at pH=6.4. Furthermore, 360 bed volumes (=3 days) after backwash at pH=7.8 the graph indicates clogging of the anthracite layer.

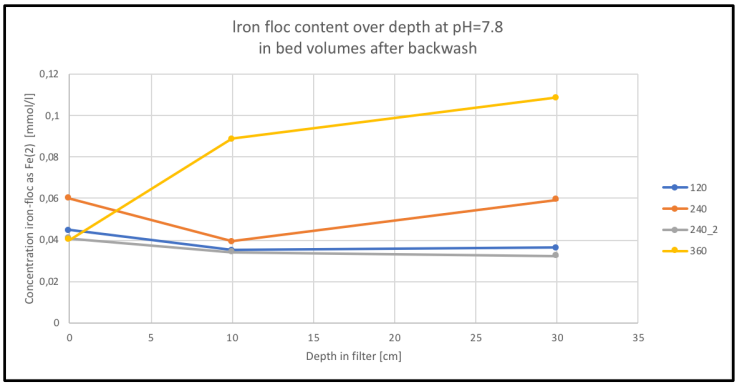

Figure 24 HFO content at pH=7.8 in Bed Volumes after backwash

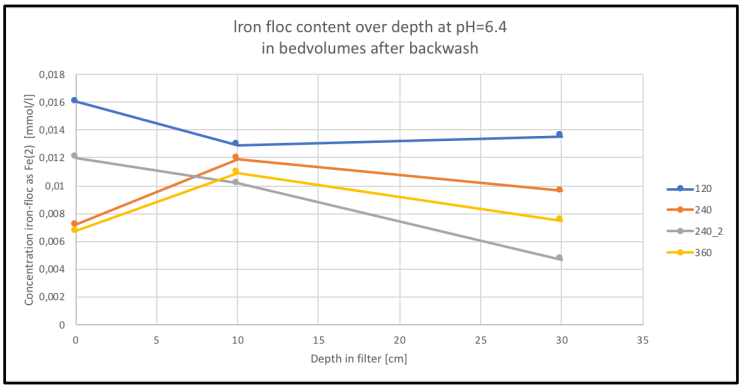

Figure 25 HFO content at pH=6.4 in Bed Volumes after backwash

Both HFO and Fe filtered concentrations are put into a text file that PHREEQC is able to read. HFO represents the mobile iron floc concentration and Fe filtered represents the dissolved ferrous iron. In PHREEQC this data is used in the graphs in order to calibrate the model.

3.3 Important parameters

The important parameters of the filter columns are included in table 2 below.

Filter	
Height, y [m]	0.4
Flow velocity, v [m/h]	5
Porosity, p_0 [-]	0.4
Diameter [m]	0.085

Table 2 Filter column design

The characteristics for anthracite can be seen in table 3 below. Initially there are some iron flocs present on the surface of these grains. Appelo et al. (2010) assumed a surface exchangeable iron content (SEIC) of 2% consisting of HFO. Anthracite has a specific surface area of 107 m^2/g (Davidson, Bryant, & Williams, 1996).

Anthracite	
Diameter, d_o [m]	0.002 – 0.004
Density, ρ_d [kg/m^3]	1500
Surface Iron Content (as HFO) [%]	2
Molar weight [g/mol]	207.25
Specific surface area [m^2/g]	107

Table 3 Characteristics of anthracite

4 Results: Enhanced PHREEQC model

In this chapter modifications to the PHREEQC model are discussed. A chronological order is chosen to explain the filtration pathway. First starting with the incoming water. Then a description is given for the processes occurring in the supernatant. Where after the solution travels through the filter medium, where adsorption, physical filtration and other processes occur. The water reaches the end of the filter column, giving the end concentration.

4.1 Starting point

For this study a PHREEQC model was developed by dr. Boris van Breukelen. This was a general filtration adsorption model, not adjusted for filtration through porous media and in this case anthracite. In Appendix B his PHREEQC model can be found. For each step in the model adjustments have been made and are described for each data block that has been used.

4.1.1 CALCULATE_VALUES

In this data block the different parameters for homo- and heterogeneous oxidation are defined as well as the filtration constant λ. Since the water temperature is 11°C the homogeneous oxidation constant is set to 8.0e^{12} (l^2 mol^{-2} atm^{-1} min^{-1}). The heterogeneous oxidation constants are used from Tamura. The filtration constant is calculated with the formulae from the previous chapter (§2.4.2) and with the use of the following parameters:

Parameter	Value	Unit	Source
k_1	9,00^{-18}	-	Lerck, 1965
v	0,00139	m/s	-
Kin. viscosity	0,0000127	m^2/s	-
d_0	0,003	m	-
k_2	1	-	Lerck, 1965
p_0	0,4	-	Assumed for anthracite
n	1	-	Yao, et al., 1971
ρ_d	3,5	kg/m^3	-
c_0	0,004	kg/m^3	-
T	288	sec	-
Y (1 layer)	0,1	m	-
σ_v	8,62E-06		Calculated from §2.4.2
α	7,50E-08		Calculated from §2.4.2
λ_0	0,0189	m^{-1}	Calculated from §2.4.2
λ	0,0189	m^{-1}	Calculated from §2.4.2
v*λ	2,62E-05	s^{-1}	Calculated from §2.4.2

Table 4 Parameters and calculation for filtration rate

Since the filtration rate is defined as:

$$\frac{\delta\sigma}{\delta t} = v\lambda c$$

The variable is the concentration at different depths in the filter. Therefore, the constant becomes v*λ, which equals 2.62e^{-5} s^{-1} and is set as k_flocs_filtration in the CALCULATE_VALUES data block, see figure 24.

```
CALCULATE_VALUES
k_homogeneous          ; -start;  10 SAVE    8.0e12     ; -end
k_heteroHFO            ; -start;  10 SAVE    73         ; -end
k_heteroSFO            ; -start;  10 SAVE    73         ; -end
k_flocs_formation      ; -start;  10 SAVE    1          ; -end
k_flocs_filtration     ; -start;  10 SAVE    2.62e-5    ; -end
END
```

Figure 26 CALCULATE VALUES data block

4.1.2 SOLUTION

The initial solution is adjusted to the incoming water from Evides (see Appendix A), with 2 mg/l ferrous iron and 20 µg/l As^{3+}. It is assumed that all the HCO_3^- in the water contributes to the alkalinity of the water. Furthermore, the water is not in equilibrium with the atmospheric oxygen, since the incoming oxygen content of the water is higher than under atmospheric conditions. In PHREEQC this is done by O(0) (the zeroth redox state of oxygen, equals dissolved oxygen), see figure 25. Furthermore, it is assumed that the pores in filter bed are filled with Evides water, before the modelling starts.

```
SOLUTION 0
and
units    mg/kgw
temp     13
pH       7.8
SI       0.19
C(4)     115      as Alkalinity
O(0)     8.8
Cl       70.2
S(6)     58
Na       45
Ca       47
Mg       7.7
N(-3)    0
Fe_two   2
As(3)    0.020
END
```

Figure 27 SOLUTION data block initial solution

4.1.3 SURFACE

Surface is defined for both adsorbed and mobile iron flocs, as well as the anthracite grains. For adsorbed and mobile iron flocs this was done by the data available from Dzombak and Morel. In the supernatant iron flocs will be formed at high pH. Since the influent concentrations are known from the lab, this information is used as input. The initial iron floc concentration is 2.5 mg/l as Fe. Since SURFACE uses the concentration of iron flocs this is transferred into $4.0e^{-3}$ g/l. The number of strong and weak surface sites can then be calculated. With 0.2 mols of weak sites per mol Fe and 0.005 mols of strong sites per mol Fe.

For the anthracite grains this was calculated manually and adjusted in the model. The calculation can be found below:

Concentration anthracite in column [mol/l]:

$$c_{anthracite} = \frac{(1 - p_0) \cdot \rho_{anthracite}}{MW_{anthracite}} = 4.3\ mol/l$$

Iron flocs on anthracite [mol/l]:

$$c_{iron\ floc} = SEIC \cdot c_{anthracite} = 0.087\ mol/l$$

$$c_{iron\ floc\ grams} = c_{iron\ floc} \cdot MW_{iron\ floc} = 7.74\ g/l$$

With SEIC being the surface extractable iron content (2%,(Appelo & Postma, 2010)). Specific surface area equals 107 m^2/g, see previous chapter. The total strong sites for anthracite then equals: 0.087*0.005 = $4.35e^{-4}$ mol sites and the total weak sites: 0.087*0.2 = $1.74e^{-2}$ mol sites.

```
SURFACE 1-6
Sfo_sOH          1.74e-2     107     7.74
Sfo_wOH          4.35e-4

Hfo_sOH          5e-17     600     0.09e-11 Dw 1e-9
Hfo_wOH          2e-15
-donnan          1e-10
-equil           1
END
```

Figure 28 SURFACE data block Anthracite and mobile floc

Mobile flocs being present in the filter before filtration starts need to be defined. Since the raw water present in the filter does not contain ferrous iron, the formation of iron flocs before filtration can be neglected. However, a small initial concentration is needed in PHREEQC to kickstart it's calculations. As can be seen in figure 26 below the iron floc concentration for mobile flocs is very low.

4.1.4 KINETICS

For the kinetic reactions occurring in the supernatant the retention time is used as a time step. Since the supernatant height is between 30 and 70 centimeters, depending on the clogging of the filter, time is set to 240 sec (4min.). The kinetic reactions that are occurring throughout the filter are defined as KINETICS 1-6, since the transport flows through six cells. In this data block all kinetic formulae are given. With the TRANSPORT term these reactions are calculated at the different bed heights as well as over runtime.

4.1.5 TRANSPORT

Transport block is adjusted to the length of the filter and bed volumes that are treated based on the lab results. One bed volume, the time needed for one drop of water to pass through the filter, equals:

$$BV = \frac{h}{v} = 288\ sec$$

Six cells are chosen for the transport.

```
TRANSPORT
-cells                  6
-lengths                0.0667
-dispersivities         0.001
-diffusion_coefficient  1.295e-9
-shifts                 760
-time_step              54
-flow_direction         forward
-boundary_conditions    flux flux
-punch_cells            1-6
-punch_frequency        6
-print_frequency        1
-multi_d                true 1e-9 0.3 0 1
-correct_disp           true
```

Figure 27 TRANSPORT datablock

Since the results from the experiment were 1, 2 and 3 days after backwash this represents 120, 240 and 360 bed volumes. In figure 28 a visual is given representing the transport processes. First the incoming water is retained for some time in the supernatant and different kinetic reactions occur, resulting in the formation of iron flocs, amongst others. This iron floc is assigned a surface and the solution is ready to be transported into the first cell of the column. Every solution in each cell of the column starts with the final solution from the precious cell. Resulting in the final effluent solution after six shifts

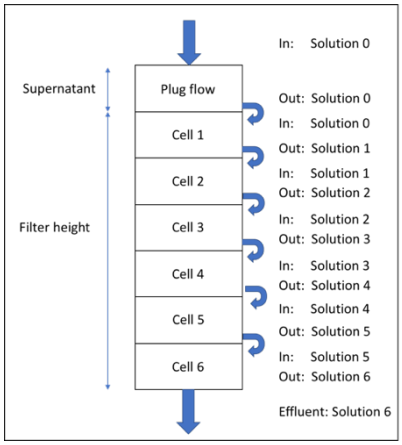

Figure 28 TRANSPORT explained

4.1.6 HEADLOSS

Due to the accumulation of iron flocs in the filter, the filter pores will clog. Clogging results in headloss over the filter. When the loss in energy becomes too high (negative) backwashing of the filter is needed, resulting in greater pore volume.

Headloss can be calculated according to Carman-Kozeny formula:

$$\frac{H_0}{L} = 180 * \frac{\vartheta}{g} * \frac{(1-p_o)^2}{{p_0}^3} * \frac{v}{{d_0}^2}$$

With:

H_0	headloss in filter [m]
L	height of filter [m]
ϑ	kinematic viscosity [m^2/s]
g	gravity constant [=9.81 m/s^2]
p_0	porosity at t=0 [-]
v	superficial flow velocity [m/s]
d_0	diameter grain [m]

In order to account for the headloss the reduction in porosity needs to be calculated per layer. This can be done with the following formulae:

$$V_{flocs\ retained} = \frac{(C_{out} - C_{in}) * A_{filter} * L_{layer}}{\rho_{flocs}}$$

$$p = p_0 * A_{filter} * L_{layer} - V_{flocs\ retained}$$

With:

$V_{flocs\ retained}$	volume of flocs retained in layer [m^3]
C_{out}	concentration of flocs flowing out of the layer [kg/m^3]
C_{in}	concentration of flocs flowing into the layer [kg/m^3]
A_{filter}	surface area of filter [m^2]
L_{layer}	height of layer [m]
ρ_{flocs}	density of flocs [kg/m^3]

p	average porosity in layer
p_0	porosity at t=0

With the average porosity of each layer, the headloss per layer and cumulative headloss can be calculated by using the above-mentioned Carman-Kozeny equation.

The headloss was modelled in PHREEQC by using the USER_GRAPH data block and enhancing this with a BASIC data block as can be seen in figure 27.

```
USER_GRAPH 2
-headings Headloss
-axis_titles Depth[m] Headloss[m] Porosity[-]
-initial_solutions false
-chart_title "Headloss over filter"
-plot_concentration_vs dist
-axis_scale x_axis 0 0.41 0.05
-axis_scale y_axis 0 1.00 0.10
-axis_scale sy_axis auto auto
-start
10 Volume_flocs = (Mobile_flocs(CELL_NO + 1) - Mobile_flocs(CELL_NO ))*89/1000 * 0.085 * 0.1 / 3.5 #Cout-Cin[kg/m3]*A[m2]*L[m]/pfloc[kg/m3]
20 Porosity =(0.4 * 0.085 * 0.1 - Volume_flocs)/(0.085*0.1) #(p0[-]*A[m2]*L[m]-Volume_flocs[m3])/A[m2]*L[m]
30 Headloss = 180*(1.15e-6/9.81)*((1-Porosity)^2/porosity^3)*(5/3600)/0.003^2*0.1 # headloss per layer, Carman-Kozeny , last numbers are L[m]
40 Tot_headloss = Headloss(CELL_NO) + Headloss(CELL_NO - 1) #cumulative headloss
100 plot_xy dist, Tot_headloss, color = red, y-axis = 1
110 plot_xy dist, Porosity, color = green, y-axis = 2
-end
```

Figure 29 Datablock Headloss

4.1.7 OUTPUT

Initially it was tried to calibrate the transport model in the lab experiments.
This was problematic because:

1. Since solutions were transported through the filter column for more than 120 times, i.e. 120 BV and six cells for each bed volume, PHREEQC struggled with performing those calculations. It took over 10 hours for the program to model for 120 BV, with six cells. Therefore, the model could not be calibrated to the experimental data.
2. Since PHREEQC had a hard time handling a high amount of bed volumes to be modeled it was chosen to model for three bed volumes. A run modelling three bed volumes took a little over 10 minutes.
3. Lab results show the concentrations for only one time sets at three different days. Mass balances were calculated for each of those moments. However, the mass balances were only valid for a short time frame. The lab results do not include continuous iron concentration measurements. Therefore, only estimates could be made for the mass balances.
4. Results from the lab had large variances between two filtration columns that were filtering under the same circumstances. The maximum error was 168% of the average concentration of the two columns and multiple concentrations had an error of >50% of the average concentration measured over two columns. Therefore, the lab results were hard to calibrate a model for, with such discrepancies in the data.

Regarding the above reasons mentioned, the choice was therefore made to model only for three bed volumes and perform an in-depth sensitivity analysis for different parameters. Furthermore, recommendations are given for new lab experiments. What data is needed and how to measure this. Below the results can be found when modelling for one, two and three bed volumes, see figures 28-31.

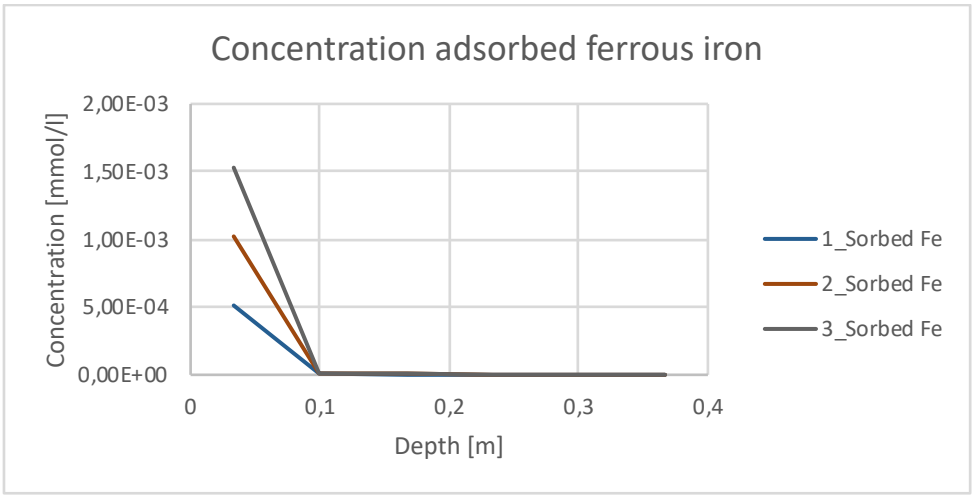

Figure 30 Concentration of adsorbed ferrous iron for 1-3 BV

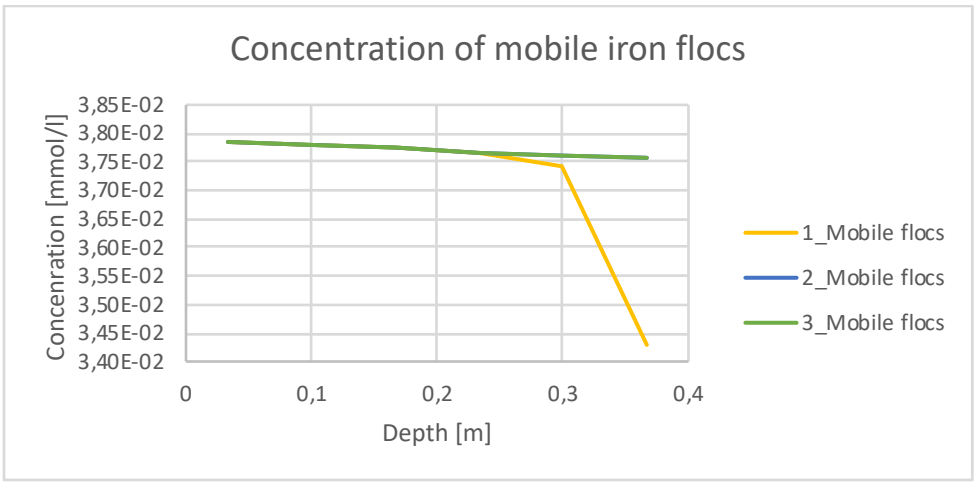

Figure 31 Concentration of mobile iron flocs for 1-3 BV

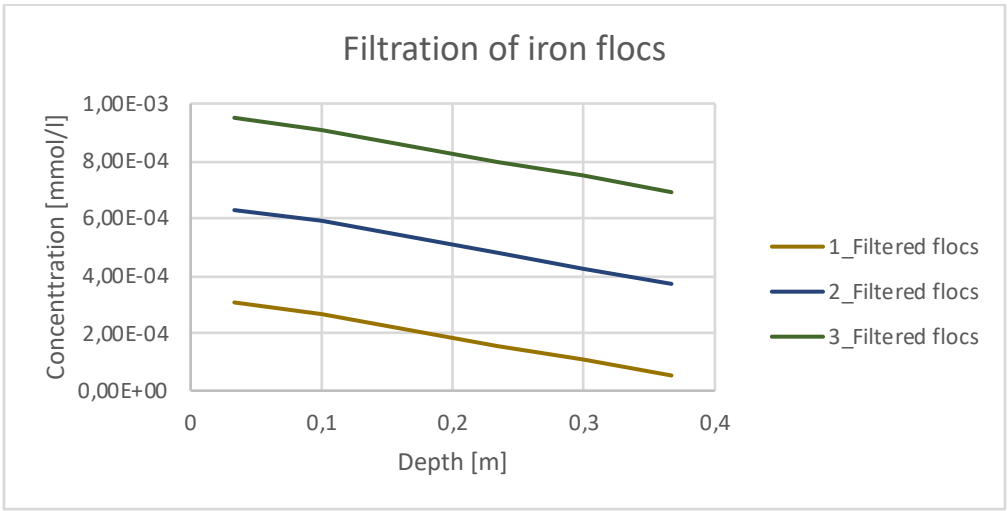

Figure 32 Filtration of iron flocs for 1-3 BV

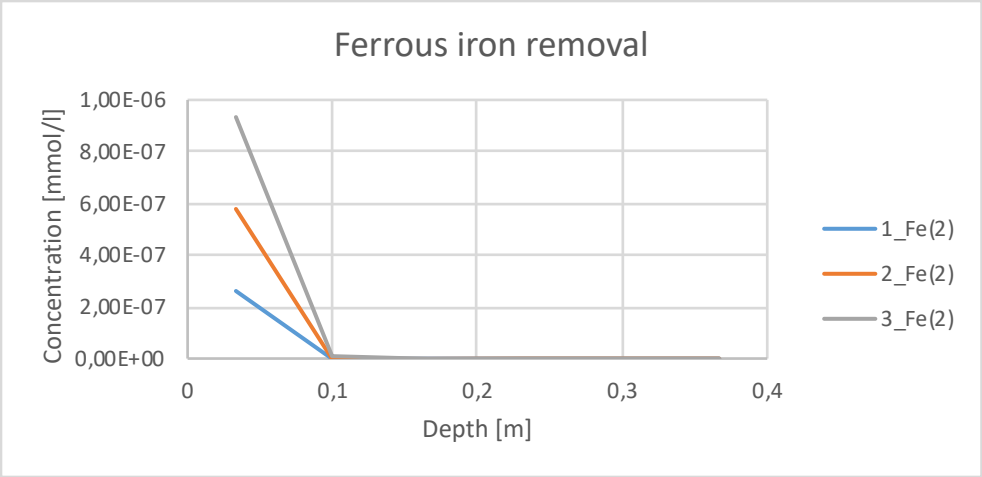

Figure 33 Ferrous iron removal for 1-3 BV

4.2 Sensitivity analysis

In order to have a more reliable model different parameters were analyzed for their sensitivity. First a standard outcome is used to calibrate. This standard is based on all the previous mentioned literature and physics and is modelled for 3 bed volumes.

4.2.1 Filtration constant

Most important and critical parameter is the filtration constant 'k_floc_filtration'. In figure 28 an overview is made for the sensitivity of this constant. The concentration of iron flocs reduces over depth, which is expected since the bigger flocs will be retained in the first part of the filter. Lowering the constant results in a very low and stable floc filtration process. The variation for the constant is based on different variations for constants like porosity and values for k_0 and n, this resulted in a range for the filtration constant between $1.0*e^{-4}$ s^{-1} and $1.0*e^{-7}$ s^{-1}. It is likely that this constant is over estimated, since it considers diffusion and PHREEQC calculates diffusion separately.

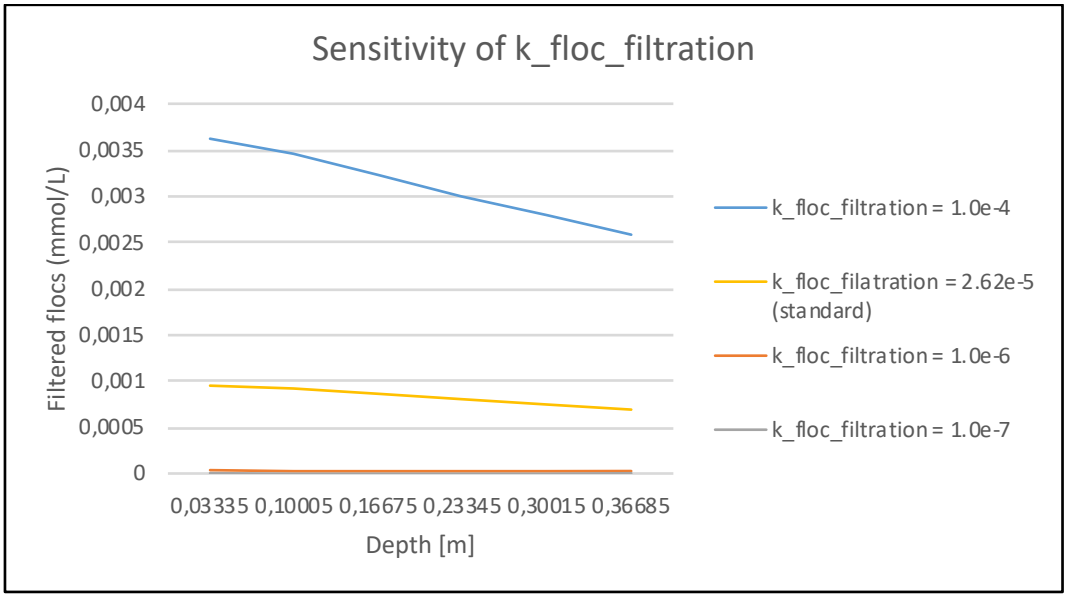

Figure 34 Sensitivity of filtration coefficient at 3 BV, pH=7

4.2.2 Surface Exchangeable Iron Content (SEIC)

Another important parameter in this filtration model is the Surface Exchangeable Iron Content (SEIC), since it influences the number of available sorption sites at the anthracite surface. As shown in figure 29, the concentration of adsorbed iron, i.e. ferrous iron adsorbed to anthracite, increases slightly for small SEIC of 0.1%. However, for 1%, 2% and 10% SEIC there is no notable difference. Also, SEIC has no influence on the concentration of filtered iron, since only very small amounts of ferrous iron are adsorbed at higher SEIC, see figure 30.

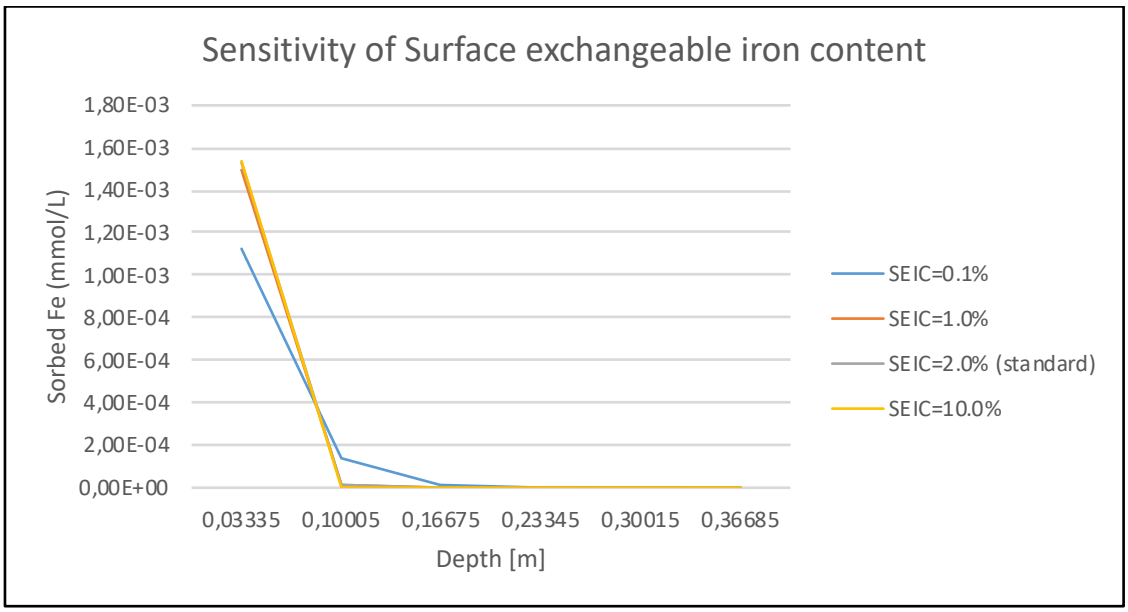

Figure 35 Sensitivity for Surface Exchangeable Iron Content at 3 BV, pH=7 for Sorbed iron

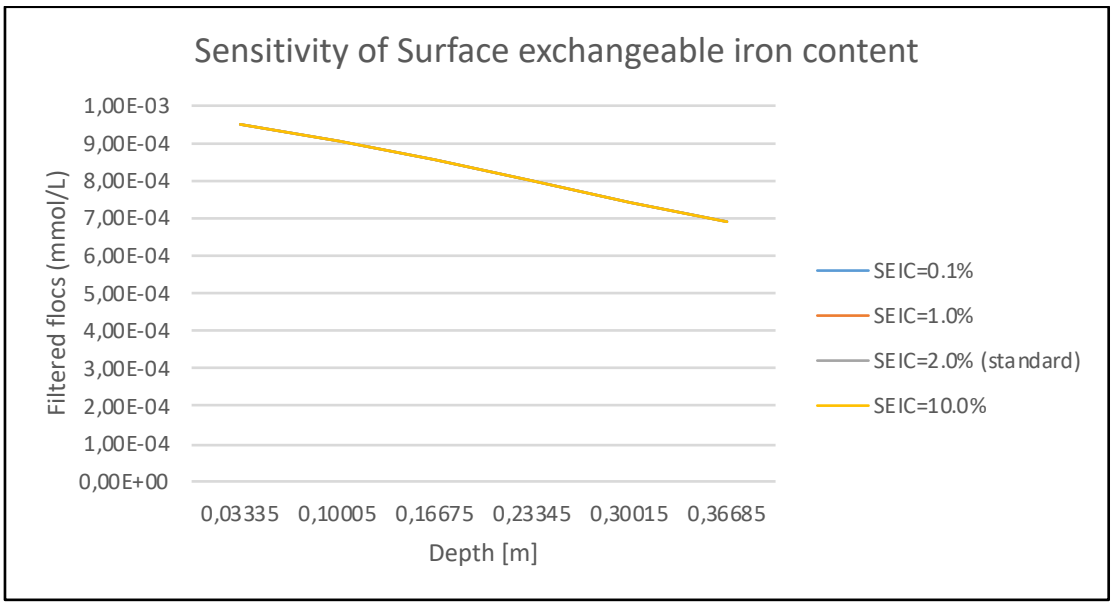

Figure 36 Sensitivity for Surface Exchangeable Iron Content at 3 BV, pH=7 for Filtered iron flocs

4.2.3 Heterogeneous oxidation constant

The constant for heterogeneous oxidation has different values in literature. Most used is Tamura's 73 mol/l/s. However, in literature a lot of discussion is found on this value. Therefore, different heterogeneous constants were modelled, between one and one hunderd. As shown in figure 31,

changing the heterogeneous oxidation constant has no effect on the overall concentration of adsorbed iron.

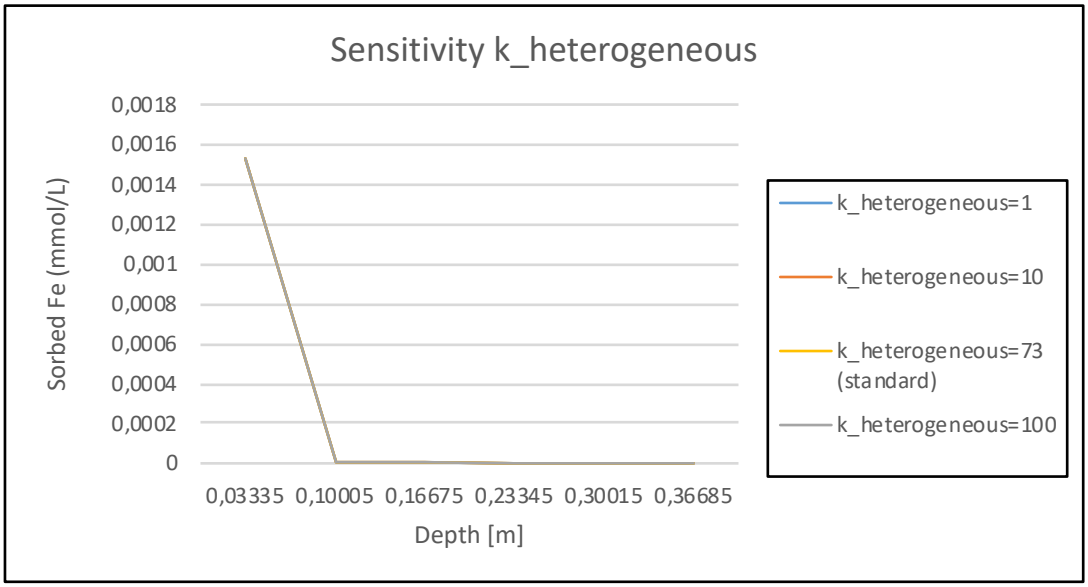

Figure 37 Sensitivity analysis for heterogeneous oxidation constant at 3 BV, pH=7

4.2.4 Diffusion coefficient

The diffusion constant D_w is another parameter influencing the model. PHREEQC needs it as input in order to have concentrations travel from one cell to another, not retaining 100 percent of the concentration in the first cell. As can be seen in figure 32, the concentration of mobile flocs does not change over depth with changing diffusion constants. It can therefore be said that the model is not very sensible to a varying diffusion.

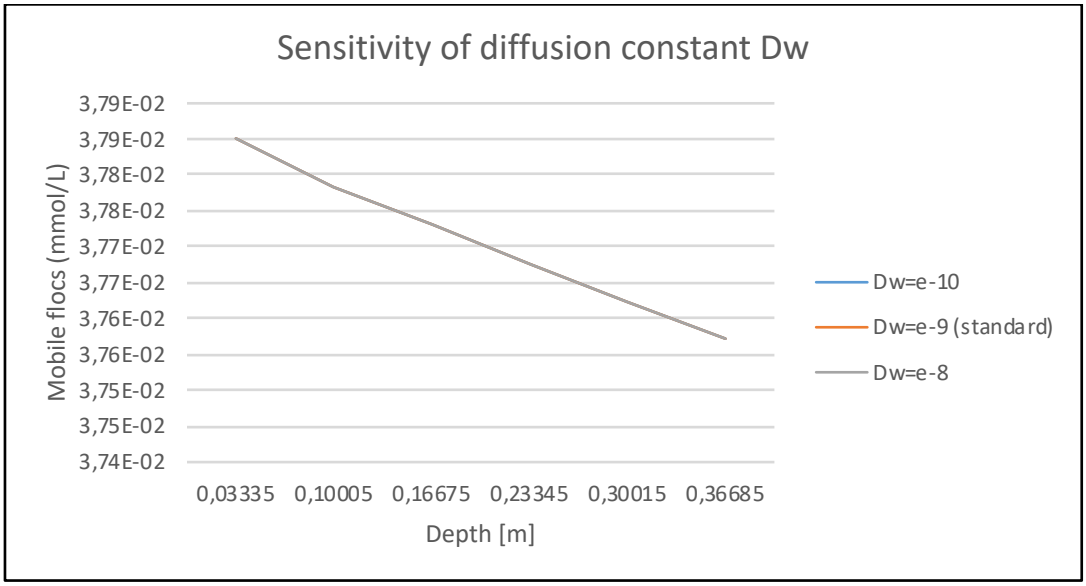

Figure 38 Sensitivity for diffusion constant Dw at 3 BV, pH=7 for mobile iron flocs

4.2.5 Retention time supernatant

The water layer on the filter, supernatant, increases with decreasing porosity, since the filter clogs by the retained iron flocs. This factor is not incorporated in this model yet. Therefore, an analysis is made

for different retention times. As can be seen in figure 33 and 34 there a lower iron floc concentration is observed with a lower retention time. This was expected, since there was less time for the homogeneous oxidation in the supernatant. However, as observed this is only a fraction compared to the standard, while the retention time is reduced by 50%, as was expected since the kinetics of homogeneous oxidation of ferrous and consequent hydrolysis occurs in a matter of (milli)seconds. Increasing the residence time has no effect on the concentration of filtered iron flocs, the ferrous iron is already fully oxidized and hydrolyzed at 240 seconds retention time.

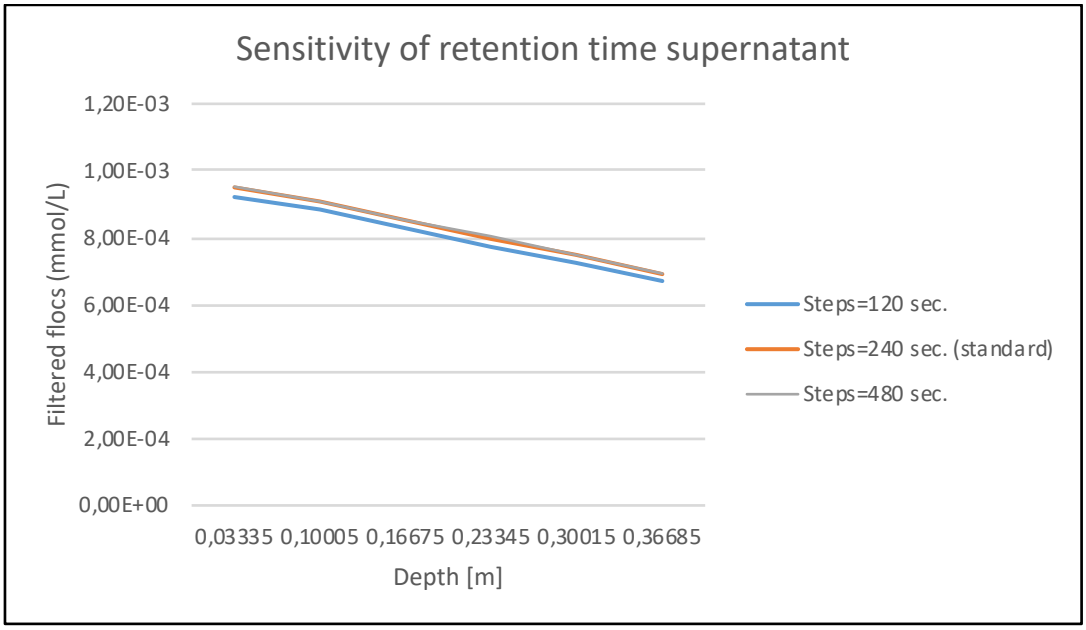

Figure 39 Sensitivity of retention time supernatant at 3 BV, pH=7 modelled for filtered iron flocs.

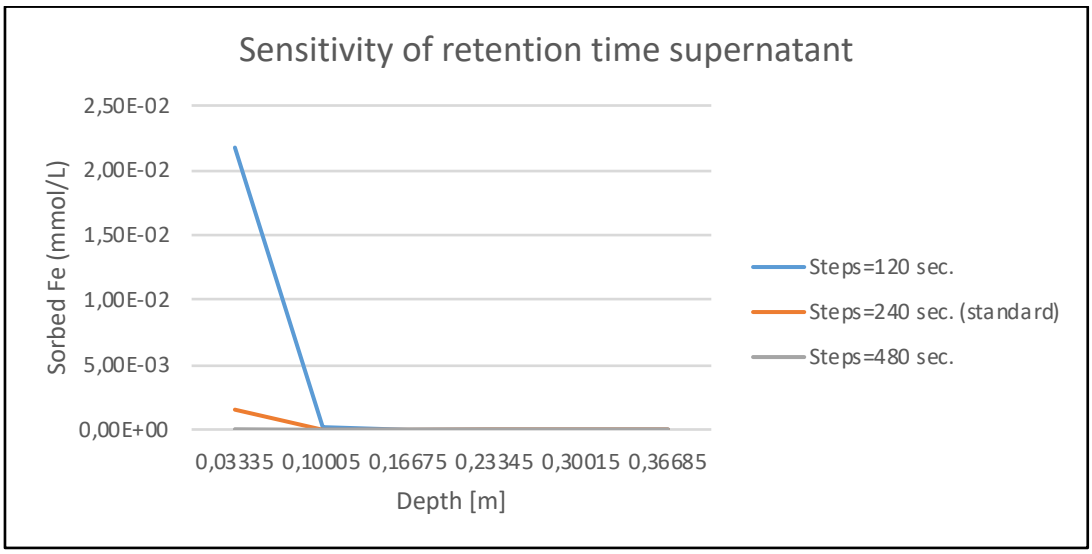

Figure 40 Sensitivity of retention time supernatant at 3 BV, pH=7 modelled for sorbed iron.

4.3 Conclusions and discussion

Overall, the performance of important parameters is adequate, as can be seen in figure 39. Some parameters show little to no difference for the overall model performance. Surface Exchangeable Iron Content, as well as the retention time of the supernatant and diffusion coefficient have a low sensitivity

for the overall performance of the model. The heterogeneous oxidation constant and diffusion coefficient show no sensitivity for the overall model performance. The filtration constant shows to be most sensitive.

Further research is recommended on the filtration constant in order to increase the reliability of the model.

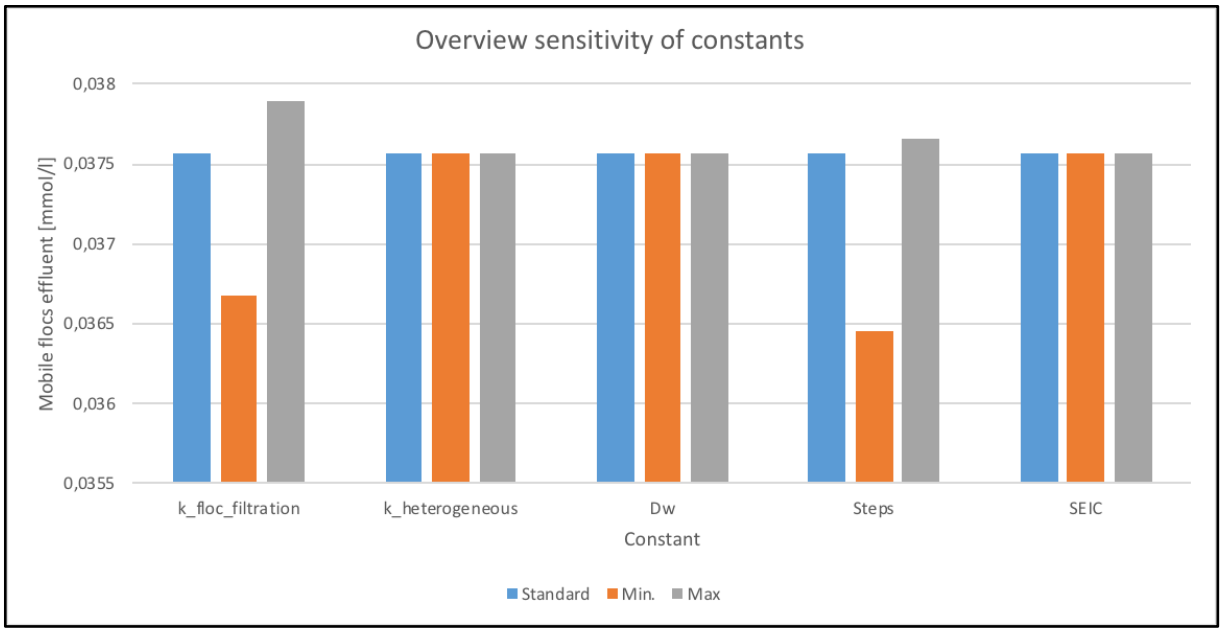

Figure 41 Overview sensitivity of constants based on the base case (standard) and their minimum and maximum sensitivity.

Further investigation into heterogeneous oxidation constant will also be critical. It is unlikely that this has no influence the overall performance of the model. One possible explanation is that there is a flow in the description of the heterogeneous oxidation in the model.

Since the diffusion coefficient does not show sensitivity for the model, it is recommended further analyze the interaction of PHREEQC with diffusion, especially through the TRANSPORT command.

5 Conclusions and recommendations

5.1 Conclusions

Though not without issues, PHREEQC can be a reasonably adequate tool to model iron floc transport. It can be used to model certain physical aspects of iron floc filtration with good results. It can also locate iron flocs in the filter column, which is highly desirable to account for arsenic adsorption on iron flocs and the depth at which this phenomenon occurs.

PHREEQC must be run over a period of several days when used to model filtration.

Sensitivity analysis highlights that the SEIC and retention time of the supernatant have low sensitivity. The diffusion coefficient and heterogeneous oxidation constant show no sensitivity to the model's performance. It is anticipated that their sensitivity is low for the model. However, no sensitivity can indicate that the heterogeneous oxidation of ferrous iron is not modelled properly, and the diffusion set in both the SURFACE and TRANSPORT commands are not working accurately.

5.2 Recommendations

Modelling iron floc filtration in rapid sand filters is a promising area of inquiry. It has the potential to deepen our insight into filter media processes and gain a more data and science driven approach towards designing, building, operating and maintaining sand filters. The modeling will increase our understanding of the filter medium, filter performance, head losses over filter height and backwash frequency. Recommendations are made below for improvements, refinements, and calibration of the model.

5.2.1 Critical improvements

The most important improvement needed is further research and refinement into and of the filtration coefficient. This variable is not the only variable in the model, and can therefore not be calibrated. It is important to investigate the influence of biological and chemical processes within this coefficient, and the importance of diffusion within this coefficient.

Diffusion as a unique coefficient needs further investigation. Since it does not show sensitivity to the model, it is possible that PHREEQC fails to account for it properly. Therefore, further research is needed into how PHREEQC interacts with and calculates diffusion in the SURFACE and TRANSPORT data blocks.

Since it takes over 10 hours to model a single day, a substantial reduction in the cycle time is important in order to analyze multiple days following a backwash. Inquiry should be made to determine whether PHREEQCP can be run through Python to reduce cycle time.

5.2.2 Lab experiments

A reliable transport model needs calibration. It is essential that the appropriate lab experiments be conducted. A recommendation is given for the set-up of this experiment, and the different data needed as output for the model.

Data needed

Additional data is required to perform a superior calibration of the model. First, the filtration columns should consist of one-meter homogeneous sand. Different parameters are required from the filter medium, see table 5.

Parameter	Unit
Density	gram/l
SEIC	mmol/gram
Porosity	-
Cation Exchange Capacity	eq/m^2

Table 5 Characteristics of sand

It is therefore recommended to measure iron concentrations at each half hour following the backwash, for a six-hour period. This will enable the startup phase of the filter to be described by the model. Furthermore, it is essential that the exact times are noted for each sample taken.

At different filter depths it is recommended to measure the following parameters, see table 6.

Parameter	Unit	Frequency (every)
Unfiltered iron	mmol/l	0.5 hours & 10cm
Filtered iron	mmol/l	0.5 hours & 10cm
Pressure	kPa	0.5 hours & 10cm
pH	-	0.5 hours & 10cm
Adsorbed iron	mmol/gram sand	day & 10 cm

Table 6 Parameters measured over filter depth

Additionally, the iron concentration of the backwash water must be measured, and an analysis of the various iron flocs released by the filter during back washing performed. This will enable the researcher to measure not only mobile flocs and ferrous iron, but make a more accurate prediction of the quantity of iron deposited in the filter bed through sedimentation.

Set up experiment

Since data from the lab experiment was not reliable, it is advisable to at least have triplicates of the columns at pH equals 6.4, 7.1 and 7.8. Furthermore, small tubes should be attached to the columns to measure the filter pressure in order to calculate head loss over time throughout the filter.

It is important that the temperature does not vary significantly because the oxidation constants are temperature dependent. This could also be solved by monitoring and controlling the temperature continuously.

Finally, the columns should be set up in such a way that the quantity of sand that can escape is negligible. This is important in order to measure the adsorption on the sand at different times and at different filter depths.

5.2.3 Improving the model

Following the implementation of the recommendations outlined above, it would be advantageous to add a biological oxidation and filtration component to the model. Decreasing porosity of the filter over time can be modelled. If properly done, the model should be able to calculate head loss over the filter using the Karman-Cozeny equation. Measuring head loss in this manner in the lab provides an additional calibration tool.

PHREEQCPy should be used to modify singular parameters. Residence time in the supernatant increases over time. However, his is a constant in the model. Furthermore, the Surface Extractable Iron Content (SEIC) of the medium depends on both the concentration of ferrous iron in the filter and runtime (S. K. Sharma, 2001). And the filtration constant is dependent on the initial iron floc

concentration in the supernatant, now the values from the lab experiment are taken as input, but it would be better if this would be included in the PHREEQCPy model as a variable as well. Modeling for these parameters through PHREEQCPy will increase model reliability.

Developing a self-learning PHREEQC model, one that defines values for the different parameters to calculate best estimates, could give an enormous boost to practical research in this area.

6 References

Appelo, C. A. J., & Postma, D. (2010). Geochemistry, Groundwater and Pollution, Second Edition. *Canadian Journal of Microbiology*, *32*(2), 678. https://doi.org/10.1201/9781439833544

Bai, R., & Tien, C. (1996). A new correlation for the initial filter coefficient under unfavorable surface interactions. *Journal of Colloid and Interface Science*, *179*(2), 631–634.

Carlson, L., & Schwertmann, U. (1980). Natural occurrence of feroxyhite (d-FeOOH). *Clays Clay Miner*, *28*, 272–280.

Cornell, R. M., & Schwertmann, U. (2003). *The iron oxides: structure, properties, reactions, occurrences and uses*. John Wiley & Sons.

Crittenden, J. C. (2012, March 14). Granular Filtration. *MWH's Water Treatment: Principles and Design, Third Edition*. https://doi.org/doi:10.1002/9781118131473.ch11

Davidson, M. I., Bryant, R., & Williams, D. J. A. (1996). Characterization of anthracite. *Geological Society, London, Special Publications*, *109*(1), 213 LP-225. Retrieved from http://sp.lyellcollection.org/content/109/1/213.abstract

Davison, W., & Seed, G. (1983). The kinetics of the oxidation of ferrous iron in synthetic and natural waters. *Geochimica et Cosmochimica Acta*, *47*(1), 67–79. https://doi.org/10.1016/0016-7037(83)90091-1

Dzombak, D. A., & Morel, F. (1990). *Surface complexation modeling: hydrous ferric oxide*. John Wiley & Sons.

Elimelech, M. (1994). Particle deposition on ideal collectors from dilute flowing suspensions: Mathematical formulation, numerical solution, and simulations. *Separations Technology*, *4*(4), 186–212.

Elimelech, M., Gregory, J., & Jia, X. (2013). *Particle deposition and aggregation: measurement, modelling and simulation*. Butterworth-Heinemann.

Goto, K., Tamura, H., & Nagayama, M. (1971). A discussion on the mechanisms of oxygenation of ferrous iron in neutral waters. *Denki Kagaku*, *39*, 690–693.

Hall, W. A. (1957). An analysis of sand filtration. *Journal of the Sanitary Engineering Division*, *83*(3), 1–9.

Huisman, L. (2004). Mechanical filtration, *2*(September), 56.

Ives, K. . (1970). Rapid filtration. *Water Research*, *4*(3), 201–223. https://doi.org/10.1016/0043-1354(70)90068-0

Iwasaki, T., Slade, J. J., & Stanley, W. E. (1937). Some notes on sand filtration [with discussion].

Journal (American Water Works Association), *29*(10), 1591–1602.

Jegatheesan, V., Vigneswaran, S., Group, E. E., & Box, P. O. (2007). Mathematical Modelling of Deep Bed Filtration, 1805–1810.

Johnson, P. R., & Elimelech, M. (1995). Dynamics of colloid deposition in porous media: Blocking based on random sequential adsorption. *Langmuir*, *11*(3), 801–812.

Keir, G., Jegatheesan, V., & Vigneswaran, S. (2009). *Deep Bed Filtration: Modelling Theory And Practice*. *Water and Wastewater Treatment Technologies*.

Kirby, C. ., Thomas, H. ., Southam, G., & Donald, R. (1999). Relative contributions of abiotic and biological factors in Fe(II) oxidation in mine drainage. *Applied Geochemistry*, *14*(4), 511–530. https://doi.org/10.1016/S0883-2927(98)00071-7

Lerck, C. (1965). Enkele aspecten van de ontijzering van grondwater.

Levich, V. G. (1962). *Physicochemical hydrodynamics.* Englewood Cliffs, N.J.: Prentice-Hall.

Maroudas, A., & Eisenklam, P. (1965). Clarification of suspensions: a study of particle deposition in granular media: Part I—Some observations on particle deposition. *Chemical Engineering Science*, *20*(10), 867–873.

Mathur, S. S. (1995). Development of a database for ion sorption on goethite using surface complexation modeling. *Carnegie Mellon University, Pittsburgh*, *14*, 15–16.

O'Melia, C. R., & Ali, W. (1979). The role of retained particles in deep bed filtration. In *Ninth International Conference on Water Pollution Research* (pp. 167–182). Elsevier.

Rajagopalan, R., & Tien, C. (1976). Trajectory analysis of deep-bed filtration with the sphere-in-cell porous media model. *AIChE Journal*, *22*(3), 523–533.

Recommendations, V. (2003). VEWIN. *The Netherlands*.

Robinson, R. B., Baumann, E. R., & Demirel, T. (1981). Identity and character of iron precipitates. *Journal of the Environmental Engineering Division*, *107*(6), 1211–1227.

Sharma, S. K. (2001). Adsorptive iron removal from groundwater. *Intemational Institute for Infrastructural, Hydraulic and Environmental Engineering*, *Master the*, 39–41.

Sharma, S., Petrusevski, B., & Schippers, J. (2005). *Biological iron removal from groundwater: A review*. *Journal of Water Supply: Research and Technology - AQUA* (Vol. 54). https://doi.org/10.2166/aqua.2005.0022

Stumm, W., & Lee, G. F. (1961). Oxygenation of Ferrous Iron. *Industrial & Engineering Chemistry*, *53*(2), 143–146. https://doi.org/10.1021/ie50614a030

Stumm, W., & Morgan, J. J. (2012). *Aquatic chemistry: chemical equilibria and rates in natural waters* (Vol. 126). John Wiley & Sons.

Sung, W., & Morgan, J. J. (1980). Kinetics and Product of Ferrous Iron Oxygenation in Aqueous Systems. *Environmental Science and Technology*, *14*(5), 561–568. https://doi.org/10.1021/es60165a006

Tamura, H., Goto, K., & Nagayama, M. (1976). The effect of ferric hydroxide on the oxygenation of ferrous ions in neutral solutions. *Corrosion Science*, *16*(4), 197–207. https://doi.org/10.1016/0010-938X(76)90046-9

Tien, C., & Payatakes, A. C. (1979). Advances in deep bed filtration. *AIChE Journal*, *25*(5), 737–759. https://doi.org/10.1002/aic.690250502

Tien, C., Turian, R. M., & Pendse, H. (1979). Simulation of the dynamic behavior of deep bed filters. *AIChE Journal*, *25*(3), 385–395. https://doi.org/10.1002/aic.690250302

Vries, D., Bertelkamp, C., Schoonenberg Kegel, F., Hofs, B., Dusseldorp, J., Bruins, J. H., … van den Akker, B. (2017). Iron and manganese removal: Recent advances in modelling treatment efficiency by rapid sand filtration. *Water Research*, *109*, 35–45. https://doi.org/10.1016/j.watres.2016.11.032

WEISS, J. (1934). Reaction Mechanism of Oxidation-Reduction Processes. *Nature*, *133*, 648. Retrieved from http://dx.doi.org/10.1038/133648c0

WHO. (2001). *Water Quality: Guidelines, Standards & Health*. IWA publishing.

Yao, K.-M., Habibian, M. T., & O'Melia, C. R. (1971). Water and waste water filtration. Concepts and applications. *Environmental Science & Technology*, *5*(11), 1105–1112. https://doi.org/10.1021/es60058a005

Productielocatie Kralingen - Gemiddelde drinkwaterkwaliteit per maand en voortschrijdend jaar

Parameter	Eenheid	Wettelijke norm minimum	Wettelijke norm maximum	APR 2017	MEI 2017	JUN 2017	JUL 2017	AUG 2017	SEP 2017	OKT 2017	NOV 2017	DEC 2017	JAN 2018	FEB 2018	MRT 2018	Gemiddeld
Temperatuur	°C	-	25	10,9	13	18,7	20,5	20	19,4	16,3	12,5	8,2	6,5	5,2	3,8	13
Zuurstof	mg/l O2	2	-	10,4	8,7	6,7	6	6,3	6,8	7,6	8,9	10	11,1	11,5	11,7	8,8
Troebeling	FTE	-	1	0,03	0,03	0,03	0,04	0,02	0,03	0,03	0,03	0,02	0,02	0,02	0,03	0,03
Geur	-	-	geen afw*	geen afw.	geen afw.	geen afw.	geen afw.	geen afw.	geen afw.	geen afw.	geen afw.	geen afw.	geen afw.	geen afw.	geen afw.	-
Smaak	-	-	geen afw.	geen afw.	geen afw.	geen afw.	geen afw.	geen afw.	geen afw.	geen afw.	geen afw.	geen afw.	geen afw.	geen afw.	geen afw.	-
Zuurgraad	pH	7	9,5	7,81	8,09	8,12	8,18	8,22	8,07	8,0	8,0	7,86	7,87	7,94	7,88	8
Verzadigingsindex	SI	-0,2	-	-0,05	0,25	0,25	0,35	0,42	0,31	0,27	0,21	0,06	0,01	0,08	0,04	0,19
Geleidingsvermogen 20°C	mS/m	-	125	46,3	47,5	47,1	47,5	49,1	50,5	51,6	51,8	50,8	49,5	47,8	46,7	48,9
Waterstofcarbonaat	mg/l HCO3	60	-	110	119	118	123	127	135	135	129	124	113	114	115	121
Chloride	mg/l Cl	-	150	68,3	66,3	65,7	65,9	67,7	73,3	75,4	74,6	76	74,9	70,9	67,2	70,2
Sulfaat	mg/l SO4	-	150	57	56	55	55	56	57	61	61	62	62	58	56	58
Natrium	mg/l Na	-	150	43	41	42	44	47	49	50	50	48	46	45	41	45
Calcium	mg/l Ca	-	-	46	45	42	44	46	48	51	46	47	45	44	47	46
Magnesium	mg/l Mg	-	-	7,8	7,5	7,2	7,9	8	8,3	8,1	7,9	7,8	7,9	7,3	7	7,7
Totale hardheid	mmol/l	1	-	1,46	1,43	1,34	1,43	1,47	1,53	1,62	1,48	1,49	1,44	1,41	1,47	1,46
Ammonium	mg/l NH4	-	0,2	<0,03	<0,03	<0,03	<0,03	<0,03	<0,03	<0,03	<0,03	<0,03	<0,03	<0,03	<0,03	<0,03
Nitraat	mg/l NO3	-	50	12,2	13,2	12,7	11,3	9,3	8,3	7	7,2	7,8	7,5	10,3	9,9	10
IJzer	µg/l Fe	-	200	<5	<5	<5	6	<5	<5	<5	<5	<5	<5	<5	<5	<5
Aluminium	µg/l Al	-	200	3	3	7	2	2	3	3	1	<1,2	<1,2	<1,2	<1,2	2
Fluoride	mg/l F	-	1	0,16	0,18	0,18	0,2	0,18	0,2	0,24	0,23	0,26	0,24	0,24	0,25	0,21
Kleurintensiteit (Pt/Co-schaal)	mg/l Pt	-	20	<2	2	2	<2	2	<2	<2	<2	3	3	3	3	2
Trihalomethanen (som)	µg/l	-	25	2,9	3	2,8	2,3	2,2	1,6	1,4	0,93	1	1,1	1,2	1,4	1,8
Bacteriën van de coligroep	KVD/100 ml	-	<1	<1	<1	<1	<1	<1	<1	<1	<1	<1	<1	<1	<1	<1
Escherichia coli	KVD/100 ml	-	<1	<1	<1	<1	<1	<1	<1	<1	<1	<1	<1	<1	<1	<1
Enterococcen	KVD/100 ml	-	<1	<1	<1	<1	<1	<1	<1	<1	<1	<1	<1	<1	<1	<1
Clostridium perf. (incl sporen)	KVD/100 ml	-	<1	<1	<1	<1	<1	<1	<1	<1	<1	<1	<1	<1	<1	<1

* geen afw. = geen afwijking
NB. In verband met de doorloop- en analysetijden in ons laboratorium lopen de gegevens doorgaans 1 tot 2 maanden achter.

Informatie over andere stoffen vindt u op onze website, gebruik hiervoor onderstaande link:

Informatie stoffen in drinkwater

Of kopieer onderstaande link in uw eigen webbrowser:

https://www.evides.nl/drinkwater/waterkwaliteit-en-hardheid/stoffen-in-drinkwater

7.2 Appendix B – PHREEQC MODEL – VAN BREUKELEN

```
# CONTINUED AS VERSION 2 BECAUSE APPARENTLY A SURFACE CANNOT BE SIMULATANEOUSLY LINKED TO (IMMOBILE) EQUILIBRIUM PHASE AND BE MOBILE

# THEREFORE: formation of Fe focs simulated kinetically and both as new dissolved iron floc species and mobile surface.


# Model on iron-oxidation and sand filtration

# Developped by Boris van Breukelen 21-09-2018

# Runs with WATER4F_SF.dat database


# First steps: only iron, arsenic and manganese to be added later

# First steps: homogenous and heterogeneous ferrous iron oxidation in water layer and sandfilter plus formation of Fe-oxide flocs

# First steps: Fe-oxide flocs are convered kinetically (for now with first-order rate constant) into immobile Fe-oxides


# To condider: increase homogeneous rate constant to account for additional biological oxidation?

# To consider: NO3 in water? FeII ox with Denitrification?


DATABASE WATEQ4F_SF_two_three.dat          # path not needed when model executed in local folder


# Definition of mobile iron floc as dissolved species

SOLUTION_MASTER_SPECIES

Iron_floc Iron_floc 0.0 1 1

SOLUTION_SPECIES

Iron_floc = Iron_floc

log_k 0.0

END


INCLUDE$ SFOproperties.dat              # phreeqc-3 function to append a text file into this input file. This file contains the properties of Sfo = sorbed HFO, see http://www.hydrochemistry.eu/exmpls/colloid.html


# BELOW ALL MODEL PARAMETER VALUES ARE LISTED:

# Then these are not needed in the corresponding kinetics blocks

CALCULATE_VALUES

k_homogeneous                ; -start;  10 SAVE    1.33e12   ; -end

k_heteroHFO                  ; -start;  10 SAVE    73        ; -end #Tamura 1976     mol/L/s

k_heteroSFO                  ; -start;  10 SAVE    73        ; -end #Tamura 1976     mol/L/s

k_flocs_formation    ; -start;  10 SAVE    1                 ; -end

k_flocs_filtration      ; -start;  10 SAVE    0.1       ; -end #Arbitrarily chosen, to vary
```

```
END

RATES
Homogeneous_Iron_Oxidation              # Singer & Stumm, 1970 # Copied from MOSHIUR MODEL
-start
10  Fe_two = TOT("Fe_two")
20  if (Fe_two < 1e-9) then goto 100
30  pP_O2 = 10^(SI("O2(g)"))
40  rate = calc_value("k_homogeneous") * (ACT("OH-"))^2 * pP_O2 * Fe_two
50  if rate > Fe_two then rate = Fe_two
60  if rate > 0.25*mol("O2") then rate = 0.25*mol("O2")
70  put(rate,1)
80  moles = rate*time
100 SAVE moles
-end

Heterogeneous_Iron_Oxidation_HFO    # Oxidation of adsorbed iron ON (MOBILE) HFO # Copied from ANDREAS model
-start
10 Fe_two = MOL("Fe_two")
20 if (Fe_two < 1e-9) then goto 100
30 Fe_two_ads = MOL("Hfo_sOFe_two+") + MOL("Hfo_wOFe_two+")# Andreas did not include the species:
Hfo_wOFe_twoOH, occurs in much smaller concentrations probabably
50 rate = calc_value("k_heteroHFO") * Fe_two_ads * MOL("O2") # Tamura1976
55  put(rate,2)
60 moles = rate*time
70 if (moles > Fe_two_ads) then moles = Fe_two_ads
100 SAVE moles
-end

Heterogeneous_Iron_Oxidation_SFO    # Oxidation of adsorbed iron ON SFO: SOLID HFO # Copied from ANDREAS model
-start
10 Fe_two = MOL("Fe_two")
20 if (Fe_two < 1e-9) then goto 100
30 Fe_two_ads = MOL("Sfo_sOFe_two+") + MOL("Sfo_wOFe_two+")# Andreas did not include the species:
Hfo_wOFe_twoOH, occurs in much smaller concentrations probabably
50 rate = calc_value("k_heteroSFO") * Fe_two_ads * MOL("O2") # Tamura1976
55  put(rate,3)
60 moles = rate*time
70 if (moles > Fe_two_ads) then moles = Fe_two_ads
```

```
100 SAVE moles
-end

Formation_Iron_Flocs
-start
10  Fe_three = tot("Fe_three")
20  if (Fe_three < 1e-9) then goto 100
40  rate = calc_value("k_flocs_formation") * SR("Fe(OH)3(a)")
50  if rate > Fe_three then rate = Fe_three
70  put(rate,4)
80  moles = rate*time
100 SAVE moles
-end

Filtration_Iron_Flocs
 -start
10 if (tot("Iron_floc") < 1e-9) then goto 100
20 rate = -calc_value("k_flocs_filtration") * tot("Iron_floc") # As start a simple first-order rate model. TO DO: must be upgraded to iron floc filtration model following state-of-the-art literature
70  put(rate,5)
80  moles = rate*time
100 SAVE moles
 -end

END

############################################################
# DEFINE UPPER WATER LAYER STARTING CHEMICAL COMPOSITION:
############################################################
SOLUTION 0
units       mg/kgw
temp        20
pH          8
Fe_two      1 mmol/kgw                  # higher for testing whether model works properly
Alkalinity  1 meq/kgw
O(0)        1 O2(g) -0.7          # arbitrarily initial O2 concentration to be changed in equilibrium with a partial pressure of O2 of 10^(-0.7) = 0.2 atm
# Complete chemical analysis below:
Cl          1 mmol/kgw                  # added for testing, used as tracer
```

```
# N(5) = nitrate = 0?

# S(6)

# Na

# K

# Ca

# Mg

END


SURFACE 0          # Defined as Hfo MOBILE HFO

          # See also Phreeqc-3 manual page 244 of PDF

                    # number strong binding sites | area per mass of surface (600 m2/g for HFO) | total mass in gram (per L) | Diffusion Coefficient > 0 to make it MOBILE. TO DO: estimate real content HFO per L water

                    # NOTE when the total mass is changed (third number) then also the total number of sites (first numbers) must be changed in proportion.

Hfo_sOH            5e-17    600    0.09e-11 Dw 1e-9 # initially very low starting concentrations are given

Hfo_wOH            2e-15

-donnan 1e-10      # for mobile surface -donan or -diffuse layer must be used. Value from Appelo

-equil  0

END


# START HOMOGENEOUS IRON OXIDATION IN UPPER LAYER:

# TO DO: more realistic is to apply Tony Appelo's CSTR approach: http://www.hydrochemistry.eu/exmpls/cstr.html

USE solution 0

USE surface 0

KINETICS 0

Homogeneous_Iron_Oxidation # As a purely chemical abiotic process

-formula   Fe_two  -1.0  O2 -0.25 H -1 Fe_three  1.0 H2O 0.5


# ALSO HETEROGENEOUS included on Fe Flocs (HFO):

# Used in Andreas Antoniou et al AG 2015. To be checked again on mass balance, but seems ok

# Tested: somehow heterogeneous rate much smaller than homogeneous rate

Heterogeneous_Iron_Oxidation_HFO    # Andreas only included the main Hfo_wOFe_two+ species. Still check equation below

-formula Hfo_wOFe_two+ -1.0          O2 -0.25  H2O -2.5  Fe_three(OH)3 1.0  Hfo_wOH 1.0          H 1.0   # Negatron 1 <= comment Andreas: meaning?


# Allow Fe Flocs to form WITH KINETIC REACTION:

Formation_Iron_Flocs                # Iron_floc = dissolved species          Formation of surface sites 0.2 mol and 0.005 mol per mol Fe(OH)3

-formula   Fe_three(OH)3 -1    Iron_floc 1                    Hfo_wOH 0.2 Hfo_sOH 0.005
```

```
-steps      10          # TO ADJUST: assumed residence time, RT, (seconds) in water layer until flow in filter. TODO: calculate RT

SAVE solution 0     # solution to be transported later into the column with the transport simulation

SAVE surface 0      # surface to be transported later into the column with the transport simulation

END
```

```
##########################################################################################################
#################

# PROCESSES IN FILTER: homogenous and heterogeneous iron oxidation forming MOBILE Fe flocs PLUS filtration of Fe
Flocs

##########################################################################################################
#################
```

```
# Initial conditions in column: equilibrium with back flush water?

SOLUTION 1-10 # ten cell column

#  TO DO: Complete as done for SOLUTION 0 above but for backflush water composition

units       mg/kgw

temp        20

pH          8           #?

Fe_two      0

Alkalinity  1 meq/kgw

O(0)        1 O2(g) -0.7        # arbitrarily initial O2 concentration to be changed in equilibrium with a partial pressure of O2 of
10^(-0.7) = 0.2 atm

# Complete chemical analysis below:

# Cl

# N(5) = nitrate = 0?

# S(6)

# Na

# K

# Ca

# Mg

END
```

```
# Define surface site of initially present Fe-oxides coated to sand grains:

# NOTE: for simplicity these are only simulated as a surface not as chemically Fe(OH)3

# NOTE: the question is whether old Fe-oxides coating sand grains have same properties (like site densities, sorption contants)
as freshly formed or recently filtrated Fe flocs

# See PHREEQC-3 Manual example 8:
```

```
SURFACE 1-10
Sfo_sOH          5e-6    600    0.09
Sfo_wOH          2e-4
Hfo_sOH          5e-17    600    0.09e-11 Dw 1e-9 # initially no flocs present PERHAPS CHANGE INTO VERY SMALL STARTING CONCENTRATION?
Hfo_wOH          2e-15
-donnan 1e-10
-equil  1
END

# TO BE CHECKED: is equilibrium with Calcite to be expected? Do sands contain Calcite?

# Define kinetic processes in filter: homogeneous and heterogeneous iron oxidation:
KINETICS 1-10
Homogeneous_Iron_Oxidation
-formula   Fe_two  -1.0  O2 -0.25 H -1 Fe_three  1.0 H2O 0.5
Heterogeneous_Iron_Oxidation_HFO
-formula Hfo_wOFe_two+ -1.0          O2 -0.25  H2O -2.5  Fe_three(OH)3 1.0  Hfo_wOH 1.0          H 1.0
Heterogeneous_Iron_Oxidation_SFO
-formula Sfo_wOFe_two+ -1.0          O2 -0.25  H2O -2.5  Fe_three(OH)3 1.0  Sfo_wOH 1.0          H 1.0
Formation_Iron_Flocs
-formula   Fe_three(OH)3 -1    Iron_floc 1                    Hfo_wOH 0.2 Hfo_sOH 0.005
Filtration_Iron_Flocs
-m0 0
-formula Iron_floc 1 Hfo_w 0.2 Hfo_s 0.005 Sfo_w -0.2 Sfo_s -0.005
END

USE solution 0
USE surface 0

# Define transport simulation in the sand filter:
TRANSPORT
-cells                  10                      # number of cells in column
-lengths          0.1                   # cell length in m. column length is 1 m = 0.1m
-dispersivities         0.001                   # in m.
-diffusion_coefficient  1.295e-9                # in m2/s
-shifts                 5                       # 50/10=5 pore volumes are modeled, column flushed 5 times
-time_step              10                      # Duration of 1 shift in s. total time = shifts*time_step.
```

```
-flow_direction          forward              # water is displaced from cell to cell towards increasing cell number
-boundary_conditions     flux flux            # flux conditions at column ends
-punch_cells             1-10                 # only plot sim results of this (last) cell number (= column outlet) to
the charts
-punch_frequency  5                           # plots every 20th shift
-print_frequency  2000                        # only prints every 2000th shift to keep output file small.
-multi_d          true 1e-9 0.3 0 1           # needed to simulate the mobile surface

USER_GRAPH 1
-headings Depth Fe Cl O2 pH
-axis_titles Depth Concentration pH
-initial_solutions false
-chart_title "Iron Removal in Sand Filter: Solutes"
-plot_concentration_vs distance
#-plot_tsv_file data.txt          # plot data from tab delimited text file
-axis_scale x_axis   0 1.01 0.1          # a b c from a to b with steps of c
-axis_scale y_axis   0 1 0.1     # Concentrations
-axis_scale sy_axis 6.5 8.5 0.5          # pH
-start
10 graph_x dist                  # depth in filter
20 graph_y (tot("Fe_two")*1e3)           # Fe in mmol/l
30 graph_y (tot("Cl")*1e3)       # Cl in mmol/l
40 graph_y (mol("O2")*1e3)   # O2 in mmol/l
80 graph_sy -la("H+")                    # In this way pH is plotted in phreeqc
-end

USER_GRAPH 2
-headings Fe(II)diss Fe_HFO Fe_SFO Fe_Filtrated Fe_Total #SI_Fe(OH)3(a)
-axis_titles Depth Concentrations Filtrated-|Total-Fe
-initial_solutions false
-chart_title "Iron Removal in Sand Filter: Fe-Flocs"
-plot_concentration_vs distance
#-plot_tsv_file data.txt          # plot data from tab delimited text file
-axis_scale x_axis   0 1.01 0.1          # a b c from a to b with steps of c
-axis_scale y_axis   0 1.1 0.1           # Concentrations
-axis_scale sy_axis 0 auto
-start
10 Fe_HFO = (tot("Iron_floc") + mol("Hfo_sOFe_two+") + mol("Hfo_wOFe_two+") + mol("Hfo_wOFe_twoOH"))*1000 # Fe in
mmol/l as mobile Fe(OH)3 plus Fe(II) sorbed to it
```

```
20 Fe_SFO = (mol("Sfo_sOFe_two+") + mol("Sfo_wOFe_two+") + mol("Sfo_wOFe_twoOH"))*1000 # Fe(II) in mmol/l sorbed to immobile Fe(OH)3

30 Fe_diss = tot("Fe_two")*1000

40 Fe_filtrated = kin("Filtration_Iron_Flocs")*1000 # Filtrated Fe(OH)3 without sorbed Fe on it.

50 Fe_TOTAL = Fe_diss + tot("Fe_three")*1000 + Fe_HFO + Fe_SFO + Fe_filtrated

110 plot_xy dist, Fe_diss, color = Red, y-axis = 1 #, symbol = Circle, symbol_size = 10, line_width = 0

120 plot_xy dist, Fe_HFO, color = Brown, y-axis = 1 #, symbol = Circle, symbol_size = 10, line_width = 0

130 plot_xy dist, Fe_SFO, color = Magenta, y-axis = 1 #, symbol = Circle, symbol_size = 10, line_width = 0

140 plot_xy dist, Fe_filtrated, color = Green, y-axis = 2 #, symbol = Circle, symbol_size = 10, line_width = 0

150 plot_xy dist, Fe_TOTAL, color = Black, y-axis = 2 #, symbol = Circle, symbol_size = 10, line_width = 0

#160 plot_xy dist, SI("Fe(OH)3(a)"), color = Blue, y-axis = 2 #, symbol = Circle, symbol_size = 10, line_width = 0

-end


# ADD GRAPH ON DERIVED WATER PRESSURES IN SYSTEM? NOTE THAT Fe_filtrated ABOVE GIVES THE ADDITIONAL CONTENT OF FE-OXIDES SORBED AND CAN BE USED AS INPUT


# ADD GRAPH ON RATES REACTIONS?


END
```